Large-scale evidence of behavioral responses and adaptation to wildfire smoke

Alexandra K. Heaney[1], Elizabeth A. Mikita[1,2], Marissa L. Childs[3], Oliver O'Brien[4], Jacob Carson[1,2], Carlos F. Gould[1,⋆]

[1]School of Public Health, University of California San Diego, La Jolla, United States [2]School of Public Health, San Diego State University, San Diego, California, United States [3]University of Washington [4]Department of Geography, University College London, London, United Kingdom

⋆ Correspondence: [cagould@health.ucsd.edu]

Significance. Whether people adapt to climate hazards or become habituated by repeated exposure is poorly understood, but is important for anticipating the costs of climate change. Using data from bikeshare rides across the US, we show that wildfire smoke reduces cycling, and large smoke events cause reductions on par with those seen during COVID-19 pandemic lockdowns. Populations with increased prior smoke exposures avoid cycling more, not less. This adaptation largely reflects within-city learning across time rather than fixed differences between cities. While avoiding outdoor activity likely reduces smoke exposures, cycling provides cardiovascular benefits and displaces car trips. The complex implications of declining cycling must be considered in assessments of smoke-related health harms and climate change adaptation planning.

Abstract. Using 371 million bikeshare trips across 12 US cities from 2010 to 2024, we find that wildfire smoke reduces urban cycling substantially and nonlinearly, and that populations with more prior smoke exposures avoid cycling more, not less — a pattern consistent with adaptation rather than habituation. Leveraging day-to-day variation in smoke in a distributed lag nonlinear model with high-dimensional fixed effects to absorb spatiotemporal confounding, we estimate that increasing from 0 µg/m^3 to 25 µg/m^3 of wildfire-attributable $PM_{2.5}$ reduces daily rides by 8.2% (95% CI: 7.2–9.3%) and increasing to 50 µg/m^3 reduces rides by 20.8% (19.0–22.7%). Wildfire smoke also shortens trip duration and distance among those who ride. Weekend trips are five times as responsive as weekday trips, consistent with recreational cycling being more deferrable than commuting. At the 90th versus 0th percentile of prior-year smoke exposure, the acute response at 25 µg/m^3 is 7.9 percentage points larger; this difference is predominantly driven by

within-city, between-year changes rather than permanent geographic differences between historically smoky and cleaner-air regions, consistent with behavioral learning rather than geographic selection. Three smoke events — the 2023 Canadian wildfire transport to the Northeast, the 2020 western fires, and the 2018 Camp Fire — produced peak daily ridership declines of 25–82%. As wildfire smoke intensifies, our results suggest populations will increasingly avoid outdoor exercise and, as cycling often offsets driving, may increase emissions of greenhouse gases and other hazardous pollutants. Consequences for physical health and the climate are not captured in existing estimates of wildfire smoke-related harms.

Introduction

Wildfire smoke has become a dominant driver of poor air quality across the United States (1). Its direct health costs are increasingly well-documented: short-term exposure to wildfire smoke elevates emergency visits and hospitalizations for a range of causes (2, 3), and long-term exposure is linked to substantial excess mortality at the population scale (4, 5, 6, 7). Evidence also links wildfire smoke to worsened mental health in smoke-affected communities (8, 9). Less documented is how people change their behavior in response to smoke, what those behavioral changes cost, and what they mean for public health. Behavioral responses fall into two categories: protective, such as running an air purifier or wearing an N95 mask, which reduces exposure while maintaining routine activities; and avoidant, such as staying indoors, which forfeits the activity to reduce exposure. Whether, how much, and who engages in each type of response determines the full behavior-related cost of smoke under future warming.

Evidence from multiple data sources documents both types of responses. A systematic review of 39 studies found that 60–90% of respondents reported at least one behavioral response during smoke events — most commonly staying indoors or reducing activity — though only a minority adopted higher-cost investments such as using air filtration or wearing masks (10, 11, 12, 13). Beyond self-reported responses, cell phone mobility, park visitation, consumer purchasing, and household spending data corroborate behavioral adjustments on smoky days: more sheltering at home, less visiting public spaces, higher demand for air purifiers and masks, and declining retail sales (14, 15, 16, 17, 18, 19, 20, 21). Although these data document varied behavioral changes to wildfire smoke, what remains less understood is 1) whether avoidant actions are decided in the moment when smoke is overhead, or in advance based on smoke forecasts, and 2) how that response evolves as populations accumulate repeated exposure.

Both knowledge gaps have bearing on projections of climate damages, with the second—whether populations adapt—being particularly consequential. Whether behavioral responses to climate hazards attenuate or intensify with repeated exposures is a central and unresolved uncertainty in climate damage estimation (22, 23). In some cases, studies have shown that repeated exposure to climate hazards like floods and heat can dampen risk perceptions over time even as the hazard intensifies (24, 25). For wildfire smoke, existing qualitative and survey evidence points in both directions: heightened perception of risk with repeated exposure in some contexts, fatigue-driven normalization of wildfire smoke in others (10, 26, 27, 28).

If populations become "habituated" to wildfire smoke and no longer take the same level of protective actions, avoidance of outdoor activities will decrease in the future at the expense of greater smoke inhalation. Adaptation would mean the opposite: more avoidance and reduced smoke inhalation, but rising behavioral costs from foregone outdoor activity that compound as wildfire smoke intensifies and populations accumulate exposures.

Here we use bikeshare data to measure how outdoor cycling responds to wildfire smoke and how that response evolves with experience. Individual rides are time-stamped and tied to specific docking stations — providing revealed-preference measures of outdoor activity at a high temporal and spatial resolution. Bikeshare ridership is sensitive to both environmental conditions and public health guidance: Heaney et al. (29) use bikeshare data to estimate nonlinear ridership responses to temperature; Bi et al. (30) document the resilience and recovery of cycling during COVID-19. Using pedestrian and bicycle counts at eight city-installed counters in Seattle, Doubleday et al. (31) find that wildfire smoke events reduced activity by 15–45%.

Bikeshare users skew young, high-income, and physically active — a demographic profile that creates competing predictions for the direction and magnitude of responses to wildfire smoke (32, 33). Higher income is associated with stronger behavioral responsiveness to air-quality hazards and greater access to substitutes such as gym memberships and private vehicles (14); on this reasoning, our sample should be more avoidant than average. But selection into outdoor cycling also reveals a preference for this mode over those same alternatives, which may make committed cyclists more reluctant to cancel trips than income alone would predict. For users at the lower-income end who rely on bikeshare as a primary mode because motorized alternatives are impractical or unaffordable (34), the expected direction runs the other way: lower access to substitutes, but also a less elastic demand for cycling as a non-discretionary trip. Ex ante the net bias in our estimates relative to the general cycling public is difficult to sign.

We assemble data on 371 million bikeshare trips across 12 US cities from 2010 to 2024, including historically high-smoke western cities and historically lower-smoke eastern cities now increasingly exposed to long-range smoke transport (Fig. 1). Average wildfire-attributable $PM_{2.5}$ has risen substantially since the early 2000s (35, 36) across the sample. Large events like the June 2023 Canadian wildfire event drive high daily wildfire-attributable $PM_{2.5}$: above 130 $\mu g/m^3$ in New York and 90 $\mu g/m^3$ in Chicago based on our estimates — unprecedented levels for these populations. We combine dock-day ridership with gridded wildfire smoke

attributable $PM_{2.5}$ from Childs et al. (35) and estimate a distributed lag nonlinear model within a high-dimensional fixed-effects panel regression. The design estimates the exposure-response relationship for daily smoke concentrations and number of cycling rides controlling for seasonality, weather, city-month-year common shocks, and all time-invariant dock characteristics.

We then stratify observed responses along several margins: weekday versus weekend ridership and by time of day. We also estimate the impacts of wildfire smoke on trip duration and distance to characterize the intensive margin — that is, whether trip characteristics change on smoky days, not just whether trips occur. To test for adaptation (i.e., if ridership responds differently to smoke exposure depending on historical exposure levels), we interact the smoke exposure-response with rolling averages of prior smoke exposure at five horizons (1 day, 7 days, 30 days, 12 months, 3 years) and decompose the modifier's variance to separate within-city temporal learning from permanent geographic differences between high-smoke and low-smoke regions.

We find that wildfire smoke reduces outdoor urban cycling substantially and nonlinearly, with most of the response materializing the day after exposure. Weekend rides declined more than five times as much due to wildfire smoke concentrations than weekday rides, consistent with recreational trips being easier to forego than ones that are plausibly work related. Consistent with long-term adaptation, populations with more prior-year wildfire smoke exposure exhibit larger behavioral responses, not smaller, and our observed adaptation signal is driven by within-city, between-year changes rather than geographic differences. Our findings show that behavioral responses lag a day behind smoke exposure and suggest that populations learn to protect themselves from novel climate hazards with more prior exposure, perhaps by learning to more routinely check air quality status.

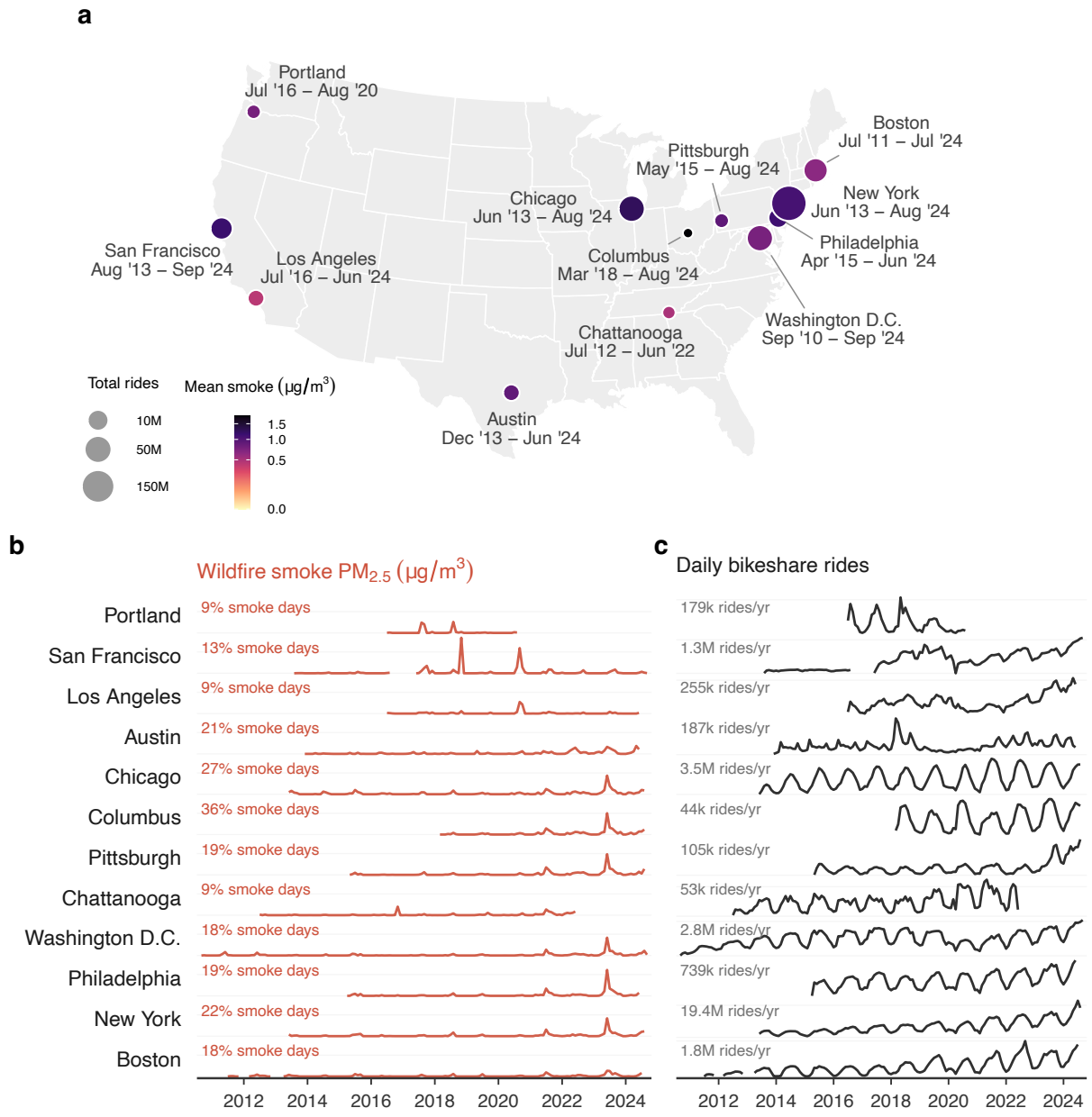

Figure 1: Bikeshare systems, rides, and wildfire smoke. (**a**) Geographic distribution of the 12 US bikeshare systems (2010–2024). Bubble size proportional to total rides; color reflects mean daily wildfire $PM_{2.5}$ from 2010-2024. (**b**) Monthly mean wildfire smoke $PM_{2.5}$ ($\mu g\,m^{-3}$) at each city. Percentage annotations indicate the fraction of days with detectable wildfire smoke ($>0\,\mu g\,m^{-3}$). (**c**) Monthly total bikeshare rides per city (y-axes differ by city). Annotations report mean annual rides over each city's observation period.

Results

Wildfire smoke nonlinearly reduces ridership

At concentrations above approximately 10 $\mu g/m^3$, increasing wildfire smoke reduces daily bikeshare ridership (Fig.2A). A day of wildfire smoke concentrations of 25 $\mu g/m^3$ reduces bikeshare ridership by 8.2% (95% CI: 7.2–9.3%) cumulatively over three days (lags 0–2). A 50 $\mu g/m^3$ day causes a 20.8% (19.0–22.7%) drop.

Examining lag-specific effects helps us to understand the timing of responses. An unconstrained lag model shows that the same-day effect at 25 $\mu g/m^3$ is near zero, while the next-day response accounts for the bulk of the cumulative estimate over the following seven days (Fig.2c,d). This pattern suggests that the behavioral response to wildfire smoke operates primarily through next-day adjustment rather than same-day reaction — consistent with either trip planning based on prior-day air quality observations or direct experience of smoke prompting cancellation of trips the following day.

At low smoke concentrations (around 5 $\mu g/m^3$), the same-day association is positive, which could be because smoke-days are on average warmer and drier than non-smoke days, conditions that are independently associated with higher ridership (Fig S4; Fig S5). Consistent with this interpretation, restricting our analysis to lags 1–7 reveals monotonically negative impacts of wildfire smoke on rides across the full smoke range.

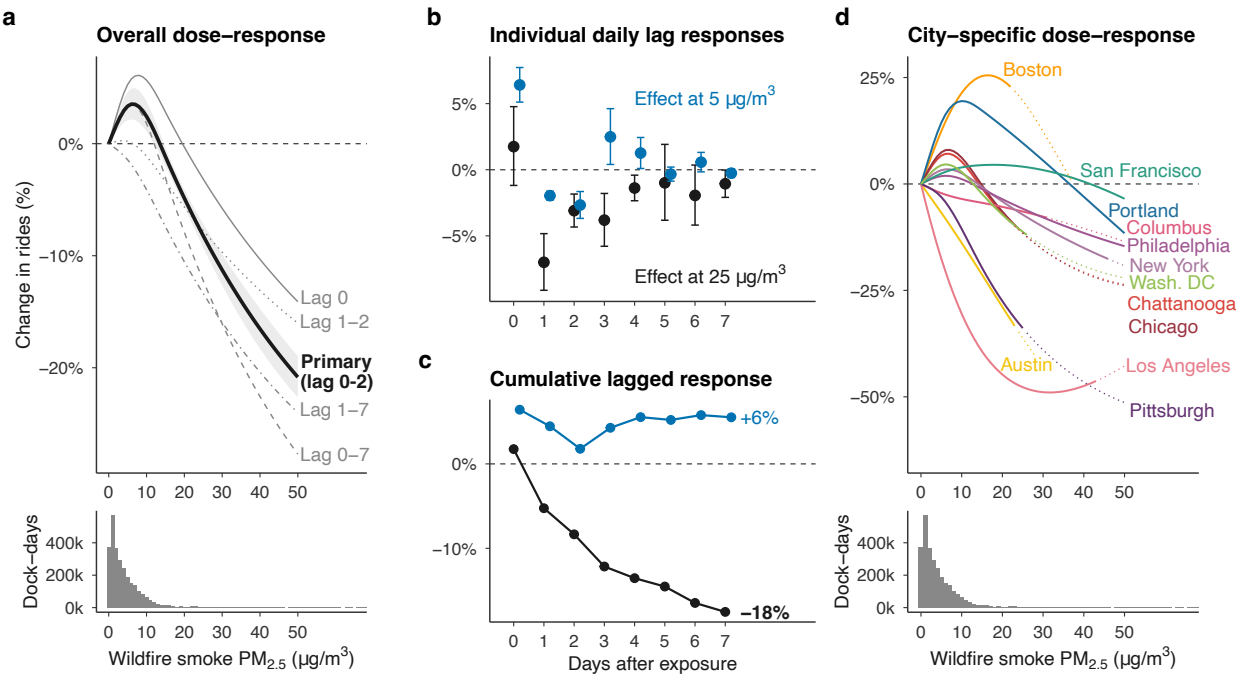

Figure 2: Wildfire smoke reduces urban cycling: primary exposure-response, city heterogeneity, and lag structure. **(a)** Cumulative exposure-response (lags 0–2) with alternative specifications labeled at 50 µg/m^3. Histogram below shows the distribution of wildfire smoke-attributable $PM_{2.5}$ on dock-days with smoke overhead. **(b)** Individual daily lagged responses at 5 and 25 µg/m^3 from an unconstrained (integer-basis) lag model. **(c)** Cumulative lagged responses at 5 and 25 µg/m^{3}from the same unconstrained (integer-basis) lag model as (b). **(d)** City-specific exposure-response curves from a two-stage meta-analysis, reported as best linear unbiased predictions (BLUPs) that shrink each city's estimate toward the pooled mean in inverse proportion to its estimation precision. Solid segments span each city's 0th–99th percentile of observed smoke days; dotted segments are to the city maximum or 50 µg/m^3.

City-specific curves, estimated via the two-stage meta-analytic approach using best linear unbiased predictions (BLUPs) (Methods), reveal both consistency and heterogeneity across the sample (Fig.2D). Nine of 12 cities show negative ridership effects at 25 µg/m^3, though for some this is beyond the 99th percentile of smoke-days (dotted segments). Among cities where 25 µg/m^3 falls within the historically observed smoke range (solid segments in Fig.2D), BLUP point estimates are mostly negative but vary widely — from +9.6% (Portland) to -47.7% (Los Angeles) — with the large eastern systems nearest the pooled effect (New York -7.2%, Philadelphia -5.8%, Washington D.C. -11.2%). Cochran's Q rejects homogeneity ($p < 0.001$), indicating meaningful between-city variation in smoke-cycling responses.

The shape of the pooled exposure-response is stable across five alternative fixed-effect structures (6.7%–11.3% decrease at 25 µg/m^3), five weather specifications (8.2%–11.5%), and four alternative spline knot placements (7.0%–8.5%; Fig S1). When modeled only during wildfire season (May–October), effects remain clearly negative, though are modestly attenuated (Fig S2).

Weekend trips are more sensitive to smoke

We stratified our main pooled model to assess weekday and weekend ridership (Fig.3a). At 25 µg/m^3, weekday ridership falls by 4.9% (95% CI: 3.4–6.3% decline), while weekend ridership falls by 24.2% (14.6–32.7%) cumulatively over two days of lags. At 50 µg/m^3, weekday ridership falls by 16.2% (13.9–18.5%) versus 33.8% (13.1–49.6%) on weekends, though weekend CIs are wide. This is consistent with discretionary weekend trips being more readily deferred than less-substitutable weekday travel, though day of week is only a coarse proxy for trip purpose.

Stratifying by four-hour departure windows reveals broadly similar responses across the day (Fig 3b; Fig S3). At 25 µg/m^3, ridership declines range from 4.3% (95% CI: 2.6–5.9%) in the Noon–4 PM window to 12.2% (9.4–14.9%) for 4–8 AM departures. At 50 µg/m^3, rides in the 4–8 AM window fall by 27.1% (21.7–32.1%) as compared to 13.5% (10.2–16.6%) from Noon–4 PM. It is possible that early-morning riders are more likely to cancel rides than those riding in the early afternoon, though, taken together, time of day appears to be a weaker discriminator of avoidance behavior than day of week.

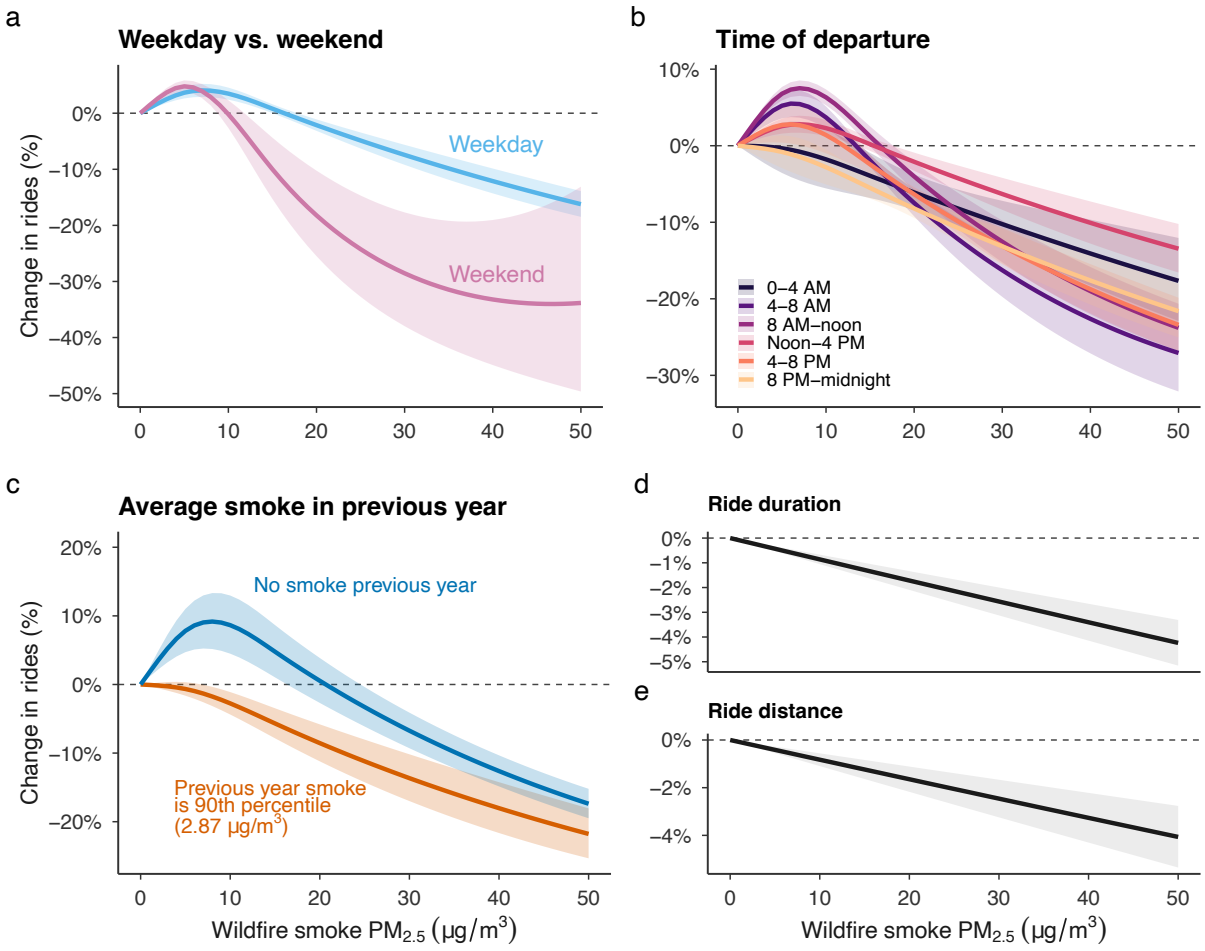

Figure 3: Heterogeneity in behavioral response by trip type, previous wildfire smoke exposures, and impacts on ride characteristics. **(a)** Impacts of wildfire smoke on weekday vs. weekend ridership in stratified models that mirror our main approach. **(b)** Stratified models by time of day of departure. **(c)** Adaptation: exposure-response at zero prior-year smoke (blue) vs. 90th percentile of 12-month rolling average (orange); 7.9 pp smoke-response difference at 25 µg/m^3. **(d, e)** Wildfire smoke effects on trip duration and distance modeled linearly.

Prior smoke exposure strengthens the avoidance response

Whether populations adapt to repeated climate hazards is an important question for projecting the costs of climate change. We test for evidence of adaptation by interacting the smoke cross-basis with a dock-level average of prior smoke exposure over various time windows (Methods). Evaluating the exposure-response at the 0th percentile of the 12-month prior-smoke modifier (zero prior-year exposure) versus the 90th percentile (2.80 $\mu g/m^3$ annual average), we find that high-prior-exposure locations exhibit larger declines in cycling across the full smoke range, with the gap between high- and low-prior-exposure locations widest at low to moderate concentrations and narrowing as concentrations increase (Fig.3C). At 25 $\mu g/m^3$, the estimated effect of smoke on rides is -3.3% (95% CI: −6.1 to −0.4) at zero prior-year exposure; at the 90th percentile, the effect is -11.2% (−14.3 to −8.0). At zero prior-year exposure, low smoke concentrations (around 5 $\mu g/m^3$) are associated with slightly increased ridership; at high prior-year exposure, the response is monotonically negative.

Evaluating the interaction across five time horizons — average wildfire smoke concentrations over the prior 1 day, prior 7 days, prior 30 days, prior 12 months, and prior 3 years — reveals that our observed adaptation is largest at one year. At 25 $\mu g/m^3$, the difference between zero prior exposure and the 90th percentile is 1.9 pp for the 1-day and 7-day modifiers, 3.7 pp for the 30-day modifier, 7.9 pp for the 12-month modifier, and 3.9 pp at the 3-year time horizon (Fig S9).

Alternative definitions for recent exposure — yesterday's smoke, current-episode length, and 3-day cumulative dose — produce little difference in their responses between high- and low-prior-exposure groups, ruling out within-episode fatigue, acute sensitization, and media-driven same-week updating as drivers of adaptation (Methods). Among other prior-year measures (e.g., smoke-day counts, highest daily smoke $PM_{2.5}$ concentration), average smoke concentration produces the largest difference between high- and low-prior-exposure groups (Methods; Fig S10).

A potential concern is that the 12-month prior-smoke modifier is higher in western cities (San Francisco, Los Angeles, Portland) which have persistently more smoke than eastern cities. If these cities differ from eastern cities in unmeasured ways that influence exposure-response — e.g., urban form, cycling infrastructure or culture, demographics, air quality awareness — the interaction could reflect permanent geographic differences rather than behavioral adaptation.

We test this directly by allowing every city its own smoke exposure-response (city-specific cross-basis slopes), so that the adaptation interaction is identified purely from within-city variation over time in prior exposure rather than from fixed differences between cities (Methods).

After absorbing each city's own dose-response, high-prior-exposure locations still respond about 2.5 pp more strongly at 10 $\mu g/m^3$ (Fig S11A), and the spread declines smoothly as between-city and then between-year variation is removed (7.9 to 5.8 to 1.9 pp at 25 $\mu g/m^3$; Fig S11B). Because the modifier is overwhelmingly within-city (95.8% of its variance; 4.2% between, 46.1% year-to-year, 49.7% across docks), this attenuation reflects how much of the effect, not the available variation, is within-city. The strictest specification has wide enough intervals to include zero on its own, but the signal points the same way throughout, peaks at the 12-month horizon, and responds only to past — not future — smoke.

Wildfire smoke shortens rides

If smoke only leads to canceled trips, the welfare cost is the foregone activity; if it also changes the character of trips that do occur, the cost extends to altered exposure and exercise intensity. We assess this by extending our primary specification to average dock-day trip duration and distance as outcomes.

Conditioning on at least one ride departing a dock, we estimate a linear exposure-response function for these outcomes (a nonlinear spline produces quantitatively similar results but with wider confidence intervals). A 25 $\mu g/m^3$ day reduces average trip duration by 2.1% (95% CI: 1.7–2.6%) and average trip distance by 2.1% (95% CI: 1.4–2.7%). Implied average speeds are essentially unchanged across the smoke distribution, indicating that riders who continue under smoke shorten their trips somewhat but maintain their typical pace.

Large smoke events produce large bikeshare disruptions

The exposure-response estimates presented above pool variation across all smoke days. To verify that these relationships translate into observable disruptions during specific, large-scale events, we estimate treatment effects around three named smoke episodes using cities that received smoke as treated units and contemporaneous clean-air cities as controls (Fig.4). We estimate average treatment effects on the treated (ATT) using the interactive fixed-effect (IFE) estimator (37), which relaxes the parallel-trends assumption by constructing city-level counterfactuals from latent factor structures fit to pre-period control cities; the number of

factors r^* is selected by cross-validation. Each of the high-profile smoke events analyzed unfolded over multiple days with highly variable day-to-day concentrations, so we report the peak single-day ATT as the key summary statistic. As a complementary estimator that does not fit a factor structure to the pre-period, we also estimate a two-way fixed effects model at the dock $\times$ day level, where date fixed effects absorb common time shocks directly; it recovers ridership changes of similar magnitude for all three events (Fig S7).

In June 2023, Canadian wildfire smoke blanketed the northeastern United States. Boston, New York, Philadelphia, and Washington D.C. experienced average smoke $PM_{2.5}$ of 52 $\mu g/m^3$on June 6, but rapidly climbed to 115 $\mu g/m^3$the next day, while West Coast cities were largely unaffected. Ridership fell sharply at onset, reaching a peak decline of 25% on day 3 (June 9), before recovering within roughly a week as smoke cleared (Fig.4a). This event is of particular interest because it exposed populations with historically low wildfire smoke experience to concentrations that western cities have faced for years, providing a window into the acute response of "naive" populations.

In September 2020, western fires drove smoke $PM_{2.5}$ to 105 $\mu g/m^3$in Los Angeles, Portland, and San Francisco against near-zero smoke in eastern cities. Ridership fell sharply, reaching a peak decline of 35% before recovering as smoke dissipated (Fig.4b).

The 2018 Camp Fire, which destroyed the town of Paradise, California, produced sustained wildfire smoke in San Francisco: concentrations reached 54 $\mu g/m^3$at onset (November 9), stayed above 50 $\mu g/m^3$for over two weeks through three distinct plume incursions, and peaked at 152 $\mu g/m^3$on November 16. Ridership dipped repeatedly across the prolonged episode, with troughs broadly tracking the successive smoke waves and reaching a peak decline of 82% (Fig.4c). With only one treated city, these estimates are imprecise and best read as illustrative of the scale of disruption rather than its exact effect.

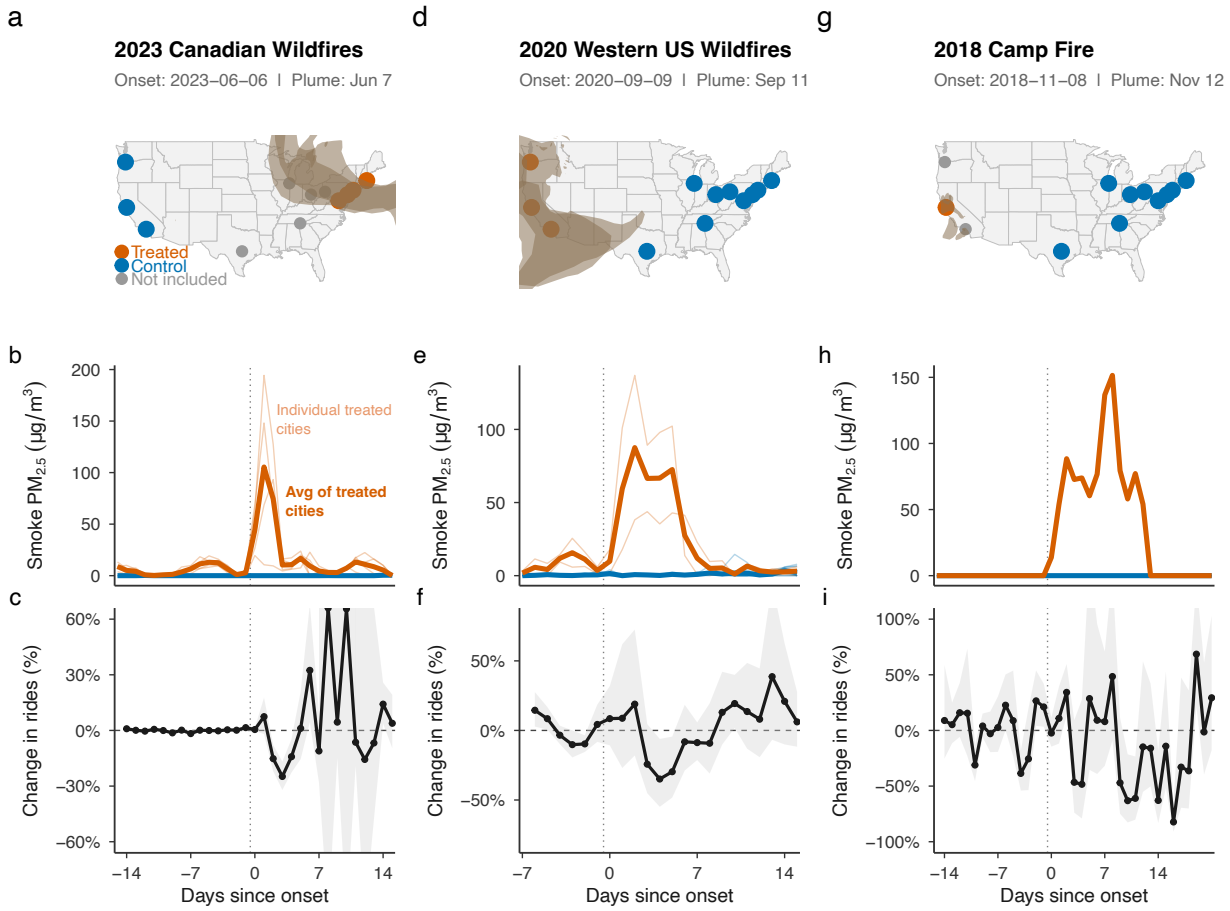

Figure 4: Large smoke events produce acute, multi-day ridership disruptions.

(a–c) Treated (orange) and control (blue) cities for each event. Overlaid smoke plumes are derived from NOAA Hazard Mapping System fire and smoke product. Grey points show cities not included in the analysis. **(d–f)** Daily wildfire smoke $PM_{2.5}$ averaged across treated and control groups; vertical line marks the date of onset. **(g–i)** Interactive fixed-effects (IFE) estimates of the average treatment effect on the treated (ATT) as percent change from the counterfactual; r^* selected by cross-validation (37). Ribbons are 95% bootstrap confidence intervals (200 draws).

Discussion

Standard health-impact assessments of wildfire smoke measure the direct cost of breathing polluted air — frequently in terms of healthcare utilization, worsened test scores, lost work days, or premature mortality (38, 21, 2, 6). Rarely measured are the indirect impacts through what people stop doing when smoke is present. Our results show that behavioral responses are large: wildfire smoke reduces outdoor cycling by 10–20% at concentrations now routinely observed during western fire seasons and increasingly during eastern transport events.

To place these effects in context: based on our data, the COVID-19 pandemic reduced bikeshare ridership across the 12-city sample by approximately 72% in the week of March 23–29, 2020 relative to the same week in 2019. The 2018 Camp Fire produced a comparable within-city disruption, recovering within two weeks of smoke clearing.

These findings place wildfire smoke alongside rising temperatures as a climate stressor that displaces and reallocates outdoor physical activity (39, 40, 41, 42, 43). Our observed adaptation implies reduced smoke inhalation by avoiding time outdoors but also potentially less exercise if individuals do not replace this activity with indoor alternatives. Decreased ridership may also increase greenhouse gas and other hazardous emissions if motor vehicle transport is used as transportation replacement. The aggregate welfare implications of this trade-off are not well represented in standard wildfire impact assessments, but are likely to grow as smoke events become more frequent and more intense under future climate change (6).

Whether repeated exposure to climate hazards breeds complacency or heightened vigilance is central to projecting the welfare costs of warming, and recent syntheses suggest the direction is not obvious a priori. For familiar hazards such as tropical cyclones, prior exposure has been shown to reduce perceived risk and willingness to take protective action over time, potentially eroding adaptive capacity even as event intensity grows (24). For wildfire smoke — a comparatively novel hazard for many newly-affected populations — survey evidence is mixed: previous experience sometimes heightens and sometimes normalizes protective behavior (10). These two futures, however, carry opposite welfare implications.

Our results speak to this ambiguity. First, most avoided rides happen the day after smoke arrives, rather than on the same day, implying that the relevant input to behavior is prior-day conditions, so advance air-quality information may be as valuable as real-time alerts for encouraging adaptive behaviors (44, 45, 17). This reliance on prior-day conditions strengthens with experience: decomposing the response into same-day (lag 0) and day-after (lag 1) com-

ponents, the day-after share of total avoidance rises from 70% at zero prior-year exposure to 92% at the 90th percentile (Fig S12), consistent with experienced populations acting increasingly on prior-day conditions rather than only same-day smoke. In agreement with this hypothesis is that the gap between experienced and inexperienced populations is largest at low-to-moderate smoke and narrows as concentrations rise. It is at deceptively moderate levels, perhaps where recognizing the hazard requires information rather than direct perception, that prior experience most changes behavior, consistent with adaptation operating through awareness and knowledge rather than physiological sensitization. Second, we find that populations with more prior-year smoke exhibit larger avoidance responses, not smaller. That this larger response peaks at the 12-month horizon — building through the prior month but largely absent at the 1-day and 7-day horizons, and flat within episodes (whether measured by consecutive smoke days, cumulative 3-day dose, or episode timing) — rules out a range of short-run mechanisms. A population habituating within a multi-day episode, a media cycle that builds over days, or a within-episode dose-loading effect would all produce modification at these finer time scales. None do. Our results instead point toward slow-moving processes that unfold over fire seasons: the gradual accumulation of risk salience as repeated smoke events update beliefs about outdoor exposure risks (46, 14, 47), the development of monitoring and communication infrastructure (17, 45, 44, 48), and growing individual investment in avoidance-enabling behaviors and resources (19, 18). That within-city, between-year variation accounts for the largest share of the adaptation signal rules out the interpretation that western cities simply differ from eastern ones.

Active transportation like bikeshare is both a climate-mitigation strategy and a source of cardiovascular and mental-health benefit (49), so smoke-driven changes in ridership bear on both climate and public health. The welfare implications of this adaptation, however, are not straightforward. On the one hand, more avoidance should reduce smoke exposure, thereby reducing smoke inhalation-related health harms. But avoidance has its own costs: foregone physical activity and active transportation carry their own health costs through reduced cardiovascular and mental health benefits, and trips that shift from cycling to car travel also carry an emissions cost. Our data do not permit us to answer whether foregone trips are replaced with other transportation options, indoor exercise, or nothing at all, and the welfare effects depend on that substitution pattern.

Adaptive capacity is not equally distributed. Lower-income populations rely disproportionately on active transportation (34, 49), have less capacity for protective investment, and face greater barriers to substituting indoor exercise alternatives (14, 10). The same adaptation

that protects wealthier populations from inhalation may displace exercise, mobility, and outdoor time most heavily among those least able to substitute. Previous evidence from the 2018 California wildfire season also points to substantial differences in avoidance behavior by education (15), suggesting one important mechanism for addressing the observed income gradient could be through targeted public health communication and smoke-awareness campaigns that reach populations with lower health literacy.

Three limitations to our analysis bear emphasis. First, we cannot identify why populations adapt. One hypothesis is that wildfire smoke becomes more salient with repeated exposure, either through individual information seeking, enhanced media coverage, or social networks. Second, we observe that trips disappear but not what they are replaced with. A foregone bikeshare trip could represent a shift to an enclosed mode (bus, subway, car), a substitution to indoor exercise, or a trip that simply does not happen. Larger ridership declines on weekends are consistent with recreational trips being more deferrable or substitutable than work-related trips, whether due to the availability of indoor alternatives, the option to forgo discretionary activity entirely, or both, but we cannot observe substitution directly. Linking bikeshare data with transit ridership, gym check-ins, or individual-level mobility traces would be needed to close this gap. Third, dock-level data cannot identify who changes behavior in response to smoke, so we cannot directly estimate distributional impacts or the role of individual characteristics (e.g., health status, income, access to information, vehicle ownership). The 12-city sample comprises larger, denser, more transit-oriented cities than the typical US city, so generalization to other settings is uncertain. That we find large avoidance responses in a population that has already revealed a strong preference for outdoor cycling over available alternatives suggests the qualitative finding is likely conservative: populations with weaker commitment to active transportation, or with fewer alternatives, may be at least as responsive to smoke, even if the precise magnitudes are population-specific.

Wildfire smoke is already displacing outdoor activity at meaningful scale, and that response increases with experience rather than fading with familiarity. This is partly good news: avoidance curbes inhaled smoke, even in the young, healthy, relatively affluent population that rides bikeshare. But avoidance is incomplete: even at 50 $\mu g/m^3$of wildfire smoke alone — more than three times the WHO 24-hour $PM_{2.5}$ guideline (50) — roughly four in five rides still happen. As smoke spreads into historically cleaner air regions and as fire seasons lengthen, the behavioral costs we document will compound rather than dissipate, and standard impact assessments that ignore them will increasingly understate the full burden of climate change (51). Whether the health-protective benefits of behavioral adaptation are broadly shared

will depend on whether information infrastructure keeps pace — and on whether avoidance remains a feasible option for those without alternatives.

Materials and Methods

Data

Bikeshare rides. We obtained individual trip records from publicly available bikeshare datasets for 12 US cities: Austin, Boston, Chattanooga, Chicago, Columbus, Los Angeles, New York City, Philadelphia, Pittsburgh, Portland, San Francisco, and Washington D.C. Trip records include departure station, arrival station, and departure time. We aggregated trips to the dock-day level (rides departing from each station on each calendar day). We classify dock-days into four categories: active with rides; true zero-demand (dock operational but no rides); system-closure (e.g., winter shutdowns where <50% of a city's docks report rides); and dock-specific outages (≥7 consecutive zero-ride days while the city was operating normally). The primary estimation sample excludes the last two groups. After panel completion, the full sample spans 2010-09-20 through 2024-09-30, comprising 14.4 million dock-days (371 million individual trips in aggregate) across 7,898 stations in 12 cities; the subset used for statistical analysis was 12.4 million dock-days. The 2 million excluded dock-days correspond to city-wide system closures (e.g., winter shutdowns in northern cities) and dock-specific outages of 7 or more consecutive zero-ride days, which we treat as non-operational rather than zero-demand. We identified and removed 128,010 exact-content duplicate journey records in three cities (Philadelphia, Los Angeles, San Francisco) arising from overlapping quarterly data files provided by the system operators. City specific docks, rides, and wildfire smoke are available in the Supplement (Figs S13–S24).

Wildfire smoke. We use daily gridded wildfire-attributable $PM_{2.5}$ from Childs et al. (35), which combines monitor data on $PM_{2.5}$ with satellite-based smoke plumes, aerosol retrievals, and other features to predict the wildfire-specific component of ambient $PM_{2.5}$ at 10 km resolution. Wildfire smoke exceeds zero on 19.6% of dock-days in the sample; among positive-smoke dock-days, the median is 2.9 $\mu g/m^3$, the 95th percentile is 13.5 $\mu g/m^3$, and 0.5% of all dock-days exceed 20 $\mu g/m^3$.

Weather. Daily maximum temperature (°C) and precipitation (mm) come from PRISM gridded climate data (4 km resolution). We include cubic polynomial terms in temperature and quadratic terms in precipitation to capture nonlinearities.

Statistical model

We estimate the effect of daily wildfire smoke $PM_{2.5}$ on dock-day ridership across all cities and docks. Our design identifies this relationship from day-to-day variation in smoke exposure within city, month, and year in the dock×day panel structure using high-dimensional fixed effects, drawing on plausibly exogenous variation driven by fire ignition timing, atmospheric transport, and wind patterns.

Our estimating equation is:

$$\log \mathbb{E}[Y_{idt}] = \alpha_i + \delta_d + \gamma_{c(i)\times m(t)} + \lambda_{c(i)\times y(t)} + f(\text{Smoke}_{it}, \text{Smoke}_{i,t-1}, \text{Smoke}_{i,t-2}) + g\big(\text{Tmx}_{it}, \text{Precip}_{it}, \text{Tmx}_{i,t-1}, \text{Precip}_{i,t-1}, \text{Tmx}_{i,t-2}, \text{Precip}_{i,t-2}\big) \quad (1)$$

where Y_{idt} is rides departing dock i on date t. Dock fixed effects α_i absorb all time-invariant station characteristics. Day-of-week fixed effects δ_d account for systematic weekly ridership patterns. City-by-month effects $\gamma_{c\times m}$ remove city-specific seasonality; city-by-year effects $\lambda_{c\times y}$ absorb differential longer-term ridership trends across cities. Together, these fixed effects ensure identification comes from day-to-day deviations in smoke exposure within dock, city, month, and year. Equation (1) is written for the primary lag window of 0–2 days; robustness checks extend $f(\cdot)$ to lags 0, 1–2, and 0–7 (see Robustness). $f(\cdot)$ is a distributed lag nonlinear function mapping smoke $PM_{2.5}$ over lags 0–2 to log ridership (see below); $g(\cdot)$ controls flexibly for weather, with polynomial terms in same-day temperature and precipitation (cubic and quadratic, respectively) plus linear terms at lags 1–2.

We estimate Eq. (1) by Poisson quasi-maximum likelihood estimation (QMLE) using the `fixest` package (52). Poisson QMLE is preferred over ordinary least squares for dock-day ride counts because the outcome is non-negative, zero-inflated (docks with zero rides on a given day), and overdispersed; the Poisson log-link implies a multiplicative exposure-response structure in which the same smoke exposure reduces ridership by a constant fraction regardless of baseline ridership level. Critically, QMLE consistency requires only correct specification of the conditional mean — not the full Poisson distributional assumption — providing robustness against overdispersion. Standard errors are clustered at the city level.

The DLNM cross-basis $f(\cdot)$ is constructed using `dlnm` (53), with natural splines in the exposure dimension (interior knots at 5 and 15 $\mu g/m^3$) and a 2-degree-of-freedom natural spline lag basis over lags 0–2 days, which constrains the lag shape to be smooth while allowing the largest effect to occur at any lag. Interior knots at 5 and 15 $\mu g/m^3$ are placed to give the spline flexibility in the two behaviorally distinct exposure regimes: the low-smoke region (<10

$\mu g/m^3$) where effects are near zero or small, and the moderate-to-high region (>15 $\mu g/m^3$) where effects steepen markedly. Placing a knot near each regime boundary allows the spline to fit the observed inflection without imposing any *a priori* monotonicity; alternative knot configurations (interior knots at 2/15, 2/25, 5/25, and 10/25 $\mu g/m^3$, single-knot placements, and a linear-in-smoke specification) do not substantively impact results (see Robustness).

We report cumulative effects: for a given smoke exposure x on day t, this is the total proportional change in ridership summed across lags 0–2, relative to a zero-smoke baseline on all days.

Robustness

We show robustness across five alternative fixed-effect structures, four lag windows (lag 0; lag 0–2; lag 1–2; lag 0–7), five weather specifications, and four alternative spline knot placements (Fig S1), as well as restricting to fire season months (May–October) (Fig S2).

Because standard errors are clustered across only $G = 12$ cities, we supplement them with the conservative t-test of Ibragimov and Müller (54), which is valid under few clusters without requiring G to be large. For each city we fit an independent city-level DLNM (same specification as the pooled model) and extract the cumulative predicted effect at a fixed smoke concentration. We apply a one-sample t-test with t_{G-1} critical values to the 12 city-specific point estimates, treating each city as one observation. This conservative test confirms a significant pooled decline at 50 $\mu g/m^3$ (-26.0%, $p < 0.001$, t_{11}) but is marginal at 25 $\mu g/m^3$ (-12.0%, $p = 0.067$), reflecting the limited power of a 12-cluster t-test; a sign test is likewise significant at 50 $\mu g/m^3$ (12/12 cities negative, $p < 0.001$) but not at 25 $\mu g/m^3$ (9/12, $p = 0.15$). Our primary clustered-SE estimates remain the basis for the headline results (Table S1).

City-specific estimates

To characterize between-city heterogeneity in smoke sensitivity, we follow the two-stage meta-analytic approach of Gasparrini et al. (53). In the first stage, we estimate city-specific DLNMs (identical specification to the pooled model but fit separately within each city). In the second stage, we pool the city-specific cross-basis coefficient vectors via multivariate random-effects meta-regression with a diagonal between-city covariance structure, yielding best linear unbiased predictions (BLUPs) of each city's exposure-response curve, shrunk toward the pooled estimate in proportion to each city's estimation precision. This approach differs from our

main, preferred pooled model, which implicitly gives more influence to cities with more dock-days and greater within-city smoke variation (e.g., New York), rather than treating each city as a single equally-weighted observation as the two-stage approach does (Fig S6 compares the pooled and two-stage exposure-response). BLUPs shrink city-specific curves with relatively few smoke days toward the pooled exposure-response while leaving cities with more wildfire smoke experience largely intact, reducing the impact of imprecise city-level estimates on the displayed heterogeneity. Cochran's Q test assesses between-city heterogeneity.

Lag structure

To examine the temporal dynamics of the behavioral response, we extend the primary lag window from 0–2 to 0–7 days and extract lag-specific (non-cumulative) predictions, i.e., the individual contribution of each lag day to the total response. We compare two specifications: a natural-spline lag basis (as in the primary model, but over 8 lags) and an unconstrained integer-basis model that places no smoothness constraint on the lag shape. The unconstrained model provides a check on whether the spline functional form biases the cumulative estimate.

Trip-type heterogeneity

We decompose the behavioral response by trip purpose using two complementary proxies. First, we fit separate DLNMs for weekday and weekend ridership. Second, we classify departures according to four hour blocks throughout the day (beginning with Midnight to 4 AM), aggregate to dock × day, and estimate separate exposure-responses. Lag 0 model results are presented in Fig S8.

Adaptation modifier

To test whether prior smoke exposure modifies the acute behavioral response, we augment the primary model with an interaction between the smoke cross-basis and a 12-month rolling average of prior smoke exposure per dock, $\overline{\text{Smoke}}^{12\text{m}}_{i,t-1}$, computed excluding the current day. The interaction is implemented by multiplying each of the six cross-basis columns by the modifier value, so the exposure-response slope and shape are both allowed to vary smoothly with prior exposure. This is a first-order (linear) interaction: the modifier enters multiplicatively with each cross-basis column, implying that the exposure-response shifts proportionally as prior smoke increases. We evaluate the exposure-response at zero prior-year exposure (0 $\mu g/m^3$) and the 90th percentile of the modifier distribution (2.80 $\mu g/m^3$).

We also evaluate the same interaction at three shorter modifier horizons (1 day, 7 days, 30 days) and one longer horizon (3 years) to distinguish acute sensitization from slow-moving learning. To further test within-episode dynamics, we refit the interaction using: yesterday's smoke $PM_{2.5}$; the number of consecutive smoke days in the current episode (capped at 5); cumulative smoke over the prior 3 days; and a binary indicator for day 2 or later of an episode. To test whether the 12-month effect is driven by chronic concentration versus event frequency, we replace the rolling average concentration with the prior-year count of heavy smoke days (>10 $\mu g/m^3$), the prior-year maximum single-day smoke, and the total count of prior-year smoke days. All models use the same cross-basis and fixed-effect structure as the primary specification. The full exposure-response overlay across all eight modifier specifications is shown in Fig S10.

Separating within-city learning from between-city differences

If our observed adaptation merely reflected fixed differences between historically smoky and historically clean cities, it would be geographic confounding rather than evidence that populations adapt over time.

A variance decomposition shows the modifier varies overwhelmingly within cities — 4.2% of its variance is between cities and 95.8% within (46.1% year-to-year, 49.7% across docks within city-year) — which establishes that within-city variation is available to identify the interaction.

We next decompose the effect itself, re-estimating the interaction on progressively demeaned modifiers: the spread between zero and 90th-percentile prior exposure at 25 $\mu g/m^3$ falls from 7.9 pp (pooled) to 5.8 pp when the modifier is city-demeaned ($Z - \bar{Z}^c$) and to 1.9 pp when it is additionally city×year-demeaned (Fig S11B). Because the demeanings are nested, these are an order-of-removal attribution rather than an orthogonal partition: removing between-city variation accounts for ≈2 pp of the spread, removing year-to-year within-city variation for a further ≈4 pp, leaving 1.9 pp from variation across docks within city-year.

Next we add city-specific cross-basis slopes (city × CB), giving each city its own full dose-response curve (which absorbs all between-city differences in the magnitude and shape of the dose-response). Because $\bar{Z}^c$ (the city-level mean of the modifier) is constant within city, the between-city interaction term $CB \times \bar{Z}^c$ is an exact linear combination of these slopes and is not separately identified, leaving the surviving interaction identified from within-city, over-time variation alone. (This is the within side of a Mundlak/correlated random-effects

decomposition (55); we do not report a separate between-city coefficient because it is not credibly identified from 12 clusters.) We find that the separation between high-exposure and low-exposure groups concentrates at low-to-moderate smoke, where it is -2.5 pp at $10\,\mu g/m^3$ (95% CI $[-6.8, +1.9]$) and attenuates to -0.7 pp at $25\,\mu g/m^3$ as the zero- and high-exposure curves nearly cross (Fig S11A). Absorbing every city-specific difference in the dose-response leaves this as a very demanding specification and a correspondingly imprecise one, so our interpretation is focused on the fact that the within-city point estimate is directionally consistent with the pooled result.

Finally, replacing prior-year with the *following* year's smoke produces no comparable modification (-1.7 pp at $25\,\mu g/m^3$ versus 9.6 pp for prior-year smoke); because smoke is serially correlated across years, this placebo is biased toward the prior-year effect, so its near-zero value is conservative and consistent with a learning interpretation in which only past exposure can shape behavior.

Event studies

To validate that the exposure-response translates into observable disruptions during specific smoke episodes, we estimate treatment effects around three named events: the Northeast smoke event of June 2023 (treated: Boston, New York, Philadelphia, Washington D.C.; controls: Los Angeles, Portland, San Francisco); the West Coast fires of September 2020 (treated: Los Angeles, Portland, San Francisco; controls: eastern and central cities); and the 2018 Camp Fire (treated: San Francisco; controls: eastern and central cities).

We estimate ATT using the IFE estimator implemented in the `fect` package (37). We aggregate rides to the city-day level and model log(rides + 1) with the same weather controls as the primary specification. The IFE estimator constructs counterfactuals by fitting r^* latent factors to pre-period control cities; r^* is selected by leave-one-out cross-validation (MSPE criterion). Pre-trend validity is assessed by inspection of pre-period coefficients. Confidence intervals use 200 bootstrap draws. We report the peak single-day ATT (most negative post-onset estimate) as the headline statistic, since the multi-day averaging window conflates the acute smoke response with post-event recovery once smoke clears.

As a robustness check we also estimate a two-way fixed effects model at the dock $\times$ day level:

$$\log \mathbb{E}[n_{idt}] = \sum_{\tau \neq -1} \beta_\tau \cdot \mathbf{1}[t = \tau] \cdot \text{Treated}_i + \gamma X_{dt} + \alpha_i + \delta_t, \tag{2}$$

where dock fixed effects α_i and date fixed effects δ_t absorb all common shocks within the window. Results from this model are shown in Fig. S7.

Intensive margin of bikeshare

Restricting to dock-days with at least one ride ($n_{\text{rides}} > 0$), we estimate the same DLNM specification on average trip duration and average network distance between departure and return dock, filtering to plausible values (duration 1–240 min, distance > 0, implied speed < 40 km/h). Network distances between bikeshare stations were calculated using the Open Source Routing Machine (OSRM; (56)), following the procedure described in its documentation. In brief, cycling distances (in kilometers) were computed for all pairwise combinations of bikeshare stations within each study city using OSRM with OpenStreetMap data, based on the network as of November 2024.

Author Contributions

AKH and CFG designed the study. EAM, OO, JC, and CFG performed analysis. All authors provided feedback on the analysis and interpretation of results. AKH, EAM, MLC, and CFG wrote the first draft of the paper with all authors providing feedback.

Acknowledgments

AKH acknowledges financial support from the National Institute of Environmental Health Sciences grant K01ES036991. JC acknowledges financial support from the National Heart, Lung, and Blood Institute grant T32HL079891. Bikeshare data supplied by the Geographic Data Service (GeoDS), a Smart Data Research UK Investment: ES/Z504464/1.

Data Availability

Bikeshare trip records are publicly available from each city's open data portal (e.g., Capital Bikeshare, Citi Bike, SFMTA Bay Wheels). Daily wildfire-attributable $PM_{2.5}$ estimates are from Childs et al. (35) and are available at https://github.com/echolab-stanford/daily-10km-smokePM. PRISM gridded climate data are freely available at https://prism.oregonstate.edu/. Analysis code and processed panel data will be deposited in a public

repository upon acceptance.

References

[1] Marissa L Childs, Jessica Li, Jeffrey Wen, Sam Heft-Neal, Anne Driscoll, Sherrie Wang, Carlos F Gould, Minghao Qiu, Jennifer Burney, and Marshall Burke. Daily local-level estimates of ambient wildfire smoke pm2. 5 for the contiguous us. *Environmental science & technology*, 56(19):13607–13621, 2022.

[2] Carlos F Gould, Sam Heft-Neal, Mary Johnson, Juan Aguilera, Marshall Burke, and Kari Nadeau. Health effects of wildfire smoke exposure. *Annual Review of Medicine*, 75(1):277–292, 2024.

[3] Colleen E. Reid, Michael Brauer, Fay H. Johnston, Michael Jerrett, John R. Balmes, and Catherine T. Elliott. Critical review of health impacts of wildfire smoke exposure. *Environmental Health Perspectives*, 124(9):1334–1343, 2016.

[4] Yiqun Ma, Emma Zang, Yang Liu, Jing Wei, Yuan Lu, Harlan M Krumholz, Michelle L Bell, and Kai Chen. Long-term exposure to wildland fire smoke pm2. 5 and mortality in the contiguous united states. *Proceedings of the National Academy of Sciences*, 121(40):e2403960121, 2024.

[5] Min Zhang, Edgar Castro, Alexandra Shtein, Adjani A Peralta, Mahdieh Danesh Yazdi, Xiao Wu, Joel D Schwartz, Robert O Wright, and Yaguang Wei. Wildfire smoke pm2. 5 and mortality rate in the contiguous united states: A causal modeling study. *Science Advances*, 12(6):eadw5890, 2026.

[6] Minghao Qiu, Jessica Li, Carlos F Gould, Renzhi Jing, Makoto Kelp, Marissa L Childs, Jeff Wen, Yuanyu Xie, Meiyun Lin, Mathew V Kiang, et al. Wildfire smoke exposure and mortality burden in the usa under climate change. *Nature*, 647(8091):935–943, 2025.

[7] Lara Schwarz, Timothy B Frankland, Sara Y Tartof, Gina S Lee, Yuqian M Gu, Elizabeth Rose Mayeda, David JX González, Tarik Benmarhnia, Joan A Casey, and Chen Chen. Long-term exposure to wildfire smoke and mortality: Heterogeneous effects by exposure metric and across subpopulations. *Proceedings of the National Academy of Sciences*, 122(51):e2509173122, 2025.

[8] Anna Humphreys, Elizabeth G Walker, Gregory N Bratman, and Nicole A Errett. What can we do when the smoke rolls in? an exploratory qualitative analysis of the impacts of rural wildfire smoke on mental health and wellbeing, and opportunities for adaptation. *BMC Public Health*, 22(1):41, 2022.

[9] David Molitor, Jamie T Mullins, and Corey White. Air pollution and suicide in rural and urban america: Evidence from wildfire smoke. *Proceedings of the National Academy of Sciences*, 120(38):e2221621120, 2023.

[10] Caroline Beckman, Isabela Miñana Lovelace, Francisca N Santana, Megan Czerwinski, Sue Anne Bell, and Alexandra Paige Fischer. A systematic review of human behavioral response to wildfire smoke. *Environmental Research Letters*, 21(1):013001, 2026.

[11] Francisca N Santana, David JX Gonzalez, and Gabrielle Wong-Parodi. Psychological factors and social processes influencing wildfire smoke protective behavior: Insights from a case study in northern california. *Climate Risk Management*, 34:100351, 2021.

[12] Lawrence A Palinkas, Jessenia De Leon, Kexin Yu, Erika Salinas, Cecilia Fernandez, Jill Johnston, Md Mostafijur Rahman, Sam J Silva, Michael Hurlburt, Rob S McConnell, et al. Adaptation resources and responses to wildfire smoke and other forms of air pollution in low-income urban settings: a mixed-methods study. *International journal of environmental research and public health*, 20(7):5393, 2023.

[13] Taylor Stewart, Alison Monroe, Katrina Mullan, Dave Jones, Abby McIver, and Ethan S Walker. Behavioral responses to wildfire smoke: a case study in western montana. *Journal of Community Health*, 50(1):31–44, 2025.

[14] Marshall Burke, Sam Heft-Neal, Jessica Li, Anne Driscoll, Patrick Baylis, Matthieu Stigler, Joakim A Weill, Jennifer A Burney, Jeff Wen, Marissa L Childs, et al. Exposures and behavioural responses to wildfire smoke. *Nature human behaviour*, 6(10):1351–1361, 2022.

[15] Clara Berestycki and M Keith Chen. Behavioral responses to wildfire smoke: Insights from smartphone location data. *Proceedings of the National Academy of Sciences*, 123(18):e2527320123, 2026.

[16] Katrina Mullan, Teigan Avery, Patrick Boise, Cindy S Leary, William L Rice, and Erin O Semmens. Impacts of wildfire-season air quality on park and playground visitation in the northwest united states. *Ecological Economics*, 224:108285, 2024.

[17] Michael Coury, Liam Falconer, and Andrea La Nauze. Wildfire smoke and private provision of public air-quality monitoring. *Journal of Environmental Economics and Management*, 127:103036, 2024.

[18] Xianru Han, Wenying Li, and Haoluan Wang. A burning issue: wildfire smoke exposure, retail sales, and demand for adaptation in healthcare. *Environmental and Resource Economics*, 87(11):3011–3039, 2024.

[19] Tamara L Sheldon and Crystal Zhan. Wildfires, smoke pollution, and household purchasing behaviors. *Journal of Economic Behavior & Organization*, 244:107474, 2026.

[20] Jacob Gellman, Margaret Walls, and Matthew Wibbenmeyer. Welfare losses from wildfire smoke: Evidence from daily outdoor recreation data. *Journal of Environmental Economics and Management*, 132:103166, 2025.

[21] Sam Heft-Neal, Carlos F Gould, Marissa L Childs, Mathew V Kiang, Kari C Nadeau, Mark Duggan, Eran Bendavid, and Marshall Burke. Emergency department visits respond nonlinearly to wildfire smoke. *Proceedings of the National Academy of Sciences*, 120(39):e2302409120, 2023.

[22] Christopher W Callahan. Present and future limits to climate change adaptation. *Nature Sustainability*, 8(4):336–342, 2025.

[23] Marshall Burke, Mustafa Zahid, Mariana CM Martins, Christopher W Callahan, Richard Lee, Tumenkhusel Avirmed, Sam Heft-Neal, Mathew Kiang, Solomon M Hsiang, and David Lobell. Are we adapting to climate change? Technical report, National Bureau of Economic Research, 2024.

[24] Gabrielle Wong-Parodi, Daniel P. Relihan, and Dana Rose Garfin. A longitudinal investigation of risk perceptions and adaptation behavior in the US Gulf Coast. *PNAS Nexus*, 3(4):pgae099, 2024.

[25] Gabrielle Wong-Parodi, Daniel P Relihan, and Dana Rose Garfin. Dynamic model of climate action. *Environmental Research Letters*, 19(9):091007, 2024.

[26] Savannah M D'Evelyn, Leah M Wood, Cody Desautel, Nicole A Errett, Kris Ray, June T Spector, and Ernesto Alvarado. Learning to live with smoke: characterizing wildland fire and prescribed fire smoke risk communication in rural washington. *Environmental Research: Health*, 1(2):025012, 2023.

[27] Catrin M Edgeley and Jack T Burnett. Understanding rural adaptation to smoke from wildfires and forest management: insights for aligning approaches with community contexts. *International journal of wildland fire*, 34(1):WF24016, 2025.

[28] Jacob Gellman and Matthew Wibbenmeyer. Wildfire smoke in the united states. *Review of Environmental Economics and Policy*, 19(1):138–150, 2025.

[29] Alexandra K Heaney, Daniel Carrión, Katrin Burkart, Corey Lesk, and Darby Jack. Climate change and physical activity: estimated impacts of ambient temperatures on bikeshare usage in new york city. *Environmental health perspectives*, 127(3):037002, 2019.

[30] Hui Bi, Zhirui Ye, Yuhan Zhang, and He Zhu. A long-term perspective on the COVID-19: the bike sharing system resilience under the epidemic environment. *Journal of Transport & Health*, 26:101460, 2022.

[31] Annie Doubleday, Youngjun Choe, Tania M Busch Isaksen, and Nicole A Errett. Urban bike and pedestrian activity impacts from wildfire smoke events in seattle, wa. *Journal of Transport & Health*, 21:101033, 2021.

[32] Amy H Auchincloss, Yvonne L Michael, Saima Niamatullah, Siyu Li, Steven J Melly, Meagan L Pharis, and Daniel Fuller. Changes in physical activity after joining a bikeshare program: a cohort of new bikeshare users. *International journal of behavioral nutrition and physical activity*, 19(1):132, 2022.

[33] Raeven Lynn M Clockston and David Rojas-Rueda. Health impacts of bike-sharing systems in the us. *Environmental research*, 202:111709, 2021.

[34] Subid Ghimire and Eleni Bardaka. Active travel among carless and car-owning low-income populations in the united states. *Transportation research part D: transport and environment*, 117:103627, 2023.

[35] Marissa Childs, Mariana Martins, Andrew Wilson, Minghao Qiu, Sam Heft-Neal, and Marshall Burke. Growing wildfire-derived pm2. 5 across the contiguous us and implications for air quality regulation. *EarthArXiv*, 2024.

[36] John T. Abatzoglou and A. Park Williams. Impact of anthropogenic climate change on wildfire across western US forests. *Proceedings of the National Academy of Sciences*, 113(42):11770–11775, 2016.

[37] Licheng Liu, Ye Wang, and Yiqing Xu. A practical guide to counterfactual estimators for causal inference with time-series cross-sectional data. *American Journal of Political Science*, 68(1):160–176, 2024. Implements the `fect` R package for IFE/gsynth estimation.

[38] Jeff Wen and Marshall Burke. Lower test scores from wildfire smoke exposure. *Nature Sustainability*, 5(11):947–955, 2022.

[39] Joshua Graff Zivin and Matthew Neidell. Temperature and the allocation of time: Implications for climate change. *Journal of Labor Economics*, 32(1):1–26, 2014.

[40] Nick Obradovich and James H Fowler. Climate change may alter human physical activity patterns. *Nature human behaviour*, 1(5):0097, 2017.

[41] Yichun Fan, Jianghao Wang, Nick Obradovich, and Siqi Zheng. Intraday adaptation to extreme temperatures in outdoor activity. *Scientific Reports*, 13(1):473, 2023.

[42] Robert I Harris. Extreme temperatures, physical activity, and adaptation. *Journal of Public Economics*, 257:105638, 2026.

[43] Christian García-Witulski, Mariano Rabassa, Oscar Melo, and Juliana Helo Sarmiento. Effects of climate change on physical inactivity: a panel data study across 156 countries from 2000 to 2022. *The Lancet Global Health*, 14(4):e500–e511, 2026.

[44] Ana G Rappold, MC Hano, S Prince, L Wei, SM Huang, C Baghdikian, B Stearns, X Gao, S Hoshiko, WE Cascio, et al. Smoke sense initiative leverages citizen science to address the growing wildfire-related public health problem. *GeoHealth*, 3(12):443–457, 2019.

[45] Morgan H. Vien, Susan L. Ivey, Hollynd Boyden, Stephanie Holm, and Linda Neuhauser. A scoping review of wildfire smoke risk communications: issues, gaps, and recommendations. *BMC Public Health*, 24:312, 2024.

[46] Christopher J Rogers, Celeste Beck, Rima Habre, and Jo Kay Ghosh. Perceived wildfire risk and past experiences with wildfire smoke influence public support for prescribed burning in the western conterminous united states. *BMC Public Health*, 25(1):102, 2025.

[47] Jacob Gellman, Margaret Walls, and Matthew Wibbenmeyer. Wildfire, smoke, and outdoor recreation in the western united states. *Forest Policy and Economics*, 134:102619, 2022.

[48] Natalie Herbert, Caroline Beckman, Cade Cannedy, Jinpu Cao, Seung-Hyun Cho, Stephanie Fischer, ShihMing Huang, Samantha J. Kramer, Ortensia Lopez, Sergio

Sanchez Lopez, et al. Improving adaptation to wildfire smoke and extreme heat in frontline communities: evidence from a community-engaged pilot study in the San Francisco Bay Area. *Environmental Research Letters*, 18:074026, 2023.

[49] Lal B Rawal, Ben J Smith, Henry Quach, and Andre MN Renzaho. Physical activity among adults with low socioeconomic status living in industrialized countries: A meta-ethnographic approach to understanding socioecological complexities. *Journal of environmental and public health*, 2020(1):4283027, 2020.

[50] World Health Organization. Who global air quality guidelines: particulate matter (pm2.5 and pm10), ozone, nitrogen dioxide, sulfur dioxide and carbon monoxide. Technical report, World Health Organization, Geneva, 2021.

[51] Solomon Hsiang, Robert Kopp, Amir Jina, James Rising, Michael Delgado, Shashank Mohan, Daniel J Rasmussen, Robert Muir-Wood, Paul Wilson, Michael Oppenheimer, et al. Estimating economic damage from climate change in the united states. *Science*, 356(6345):1362–1369, 2017.

[52] Laurent R Bergé, Kyle Butts, and Grant McDermott. Fast and user-friendly econometrics estimations: The r package fixest. *arXiv preprint arXiv:2601.21749*, 2026.

[53] Antonio Gasparrini. Distributed lag linear and non-linear models in R: the package dlnm. *Journal of Statistical Software*, 43(8):1–20, 2011.

[54] Rustam Ibragimov and Ulrich K. Müller. t-statistic based correlation and heterogeneity robust inference. *Journal of Business & Economic Statistics*, 28(4):453–468, 2010.

[55] Yair Mundlak. On the pooling of time series and cross section data. *Econometrica*, 46(1):69–85, 1978.

[56] Dennis Luxen and Christian Vetter. Real-time routing with openstreetmap data. In *Proceedings of the 19th ACM SIGSPATIAL International Conference on Advances in Geographic Information Systems*, GIS '11, pages 513–516, New York, NY, USA, 2011. ACM.

Supplementary Information

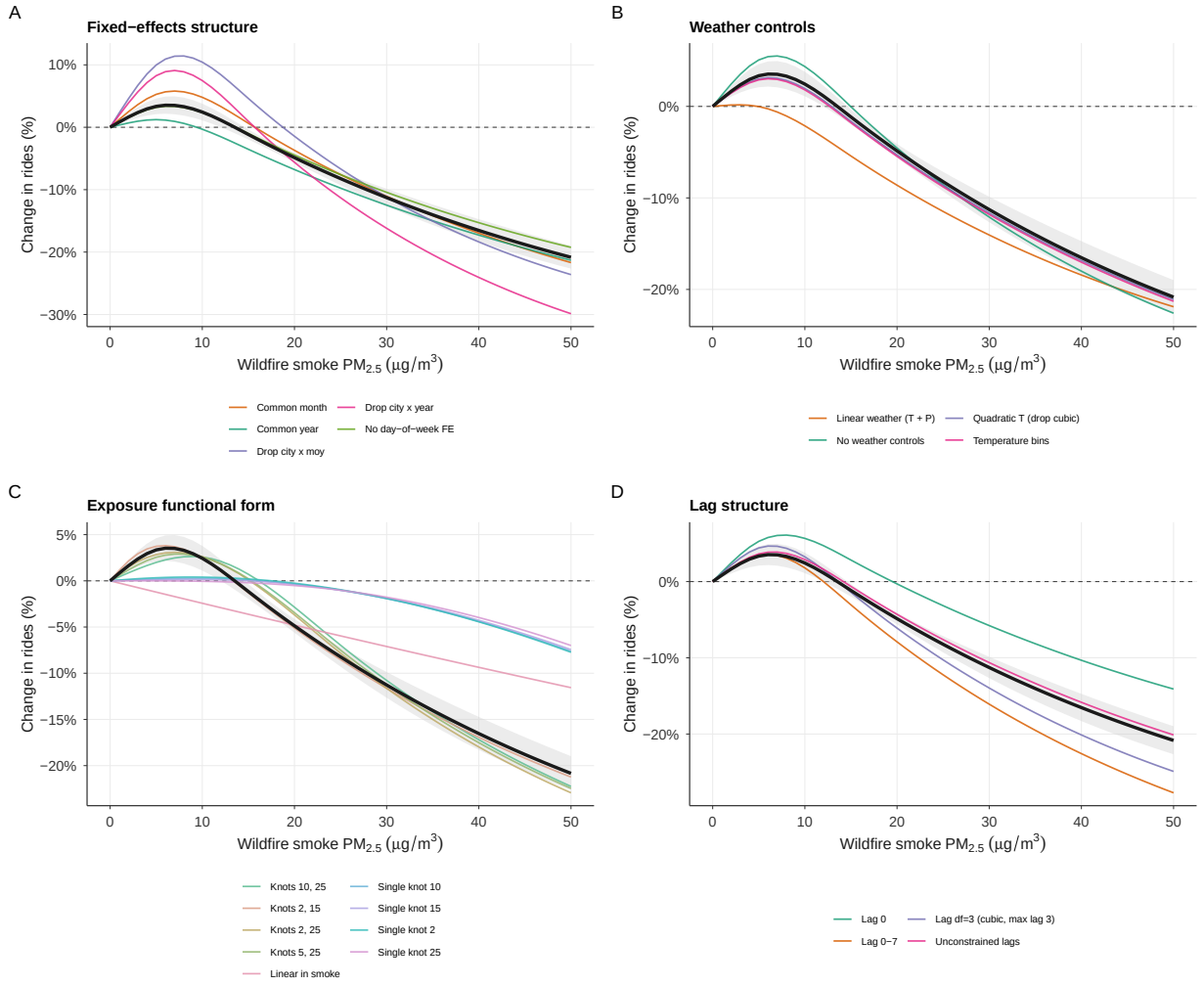

Figure S1: Full specification robustness across four dimensions. Each panel shows the cumulative exposure-response under the primary specification (bold black, with 95% CI shaded) alongside alternative specifications. The main specification includes dock, day-of-week, city×month, and city×year fixed effects; cubic temperature and quadratic precipitation controls with linear lags 1–2; and a natural spline smoke cross-basis with interior knots at 5 and 15 µg/m^3 over lags 0–2 days. **(A)** Fixed-effects robustness: five alternative FE structures; estimates at 25 µg/m^3 range from −6.7% to −11.3%. **(B)** Weather controls: five specifications; estimates at 25 µg/m^3 range from −8.2% to −11.5%. **(C)** Exposure functional form: alternative knot placements and linear-in-smoke. **(D)** Lag structure: lag 0, 0–2, 1–2, 0–7, lag df=3, and unconstrained integer-basis. Across all four dimensions the exposure-response keeps its shape and magnitude, indicating the primary estimate is not sensitive to these modeling choices.

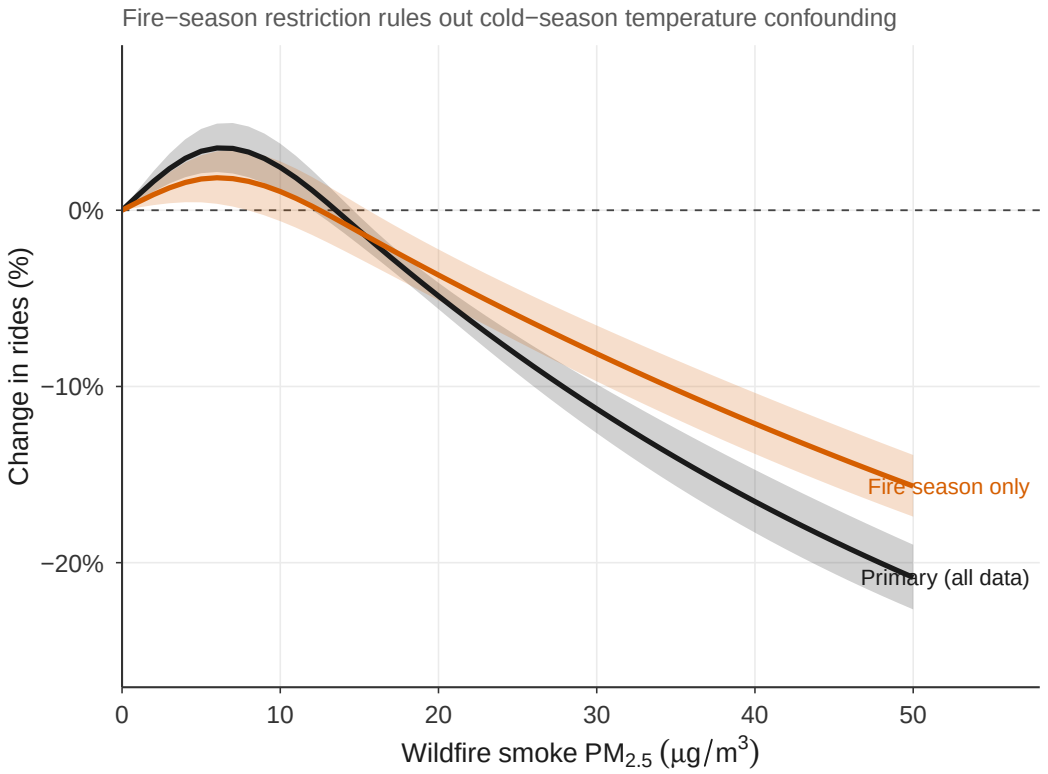

Figure S2: Fire-season robustness. Primary exposure-response (grey dashed) versus fire-season-restricted (May–October; black). Restricting to wildfire-season months leaves the response clearly negative but modestly smaller.

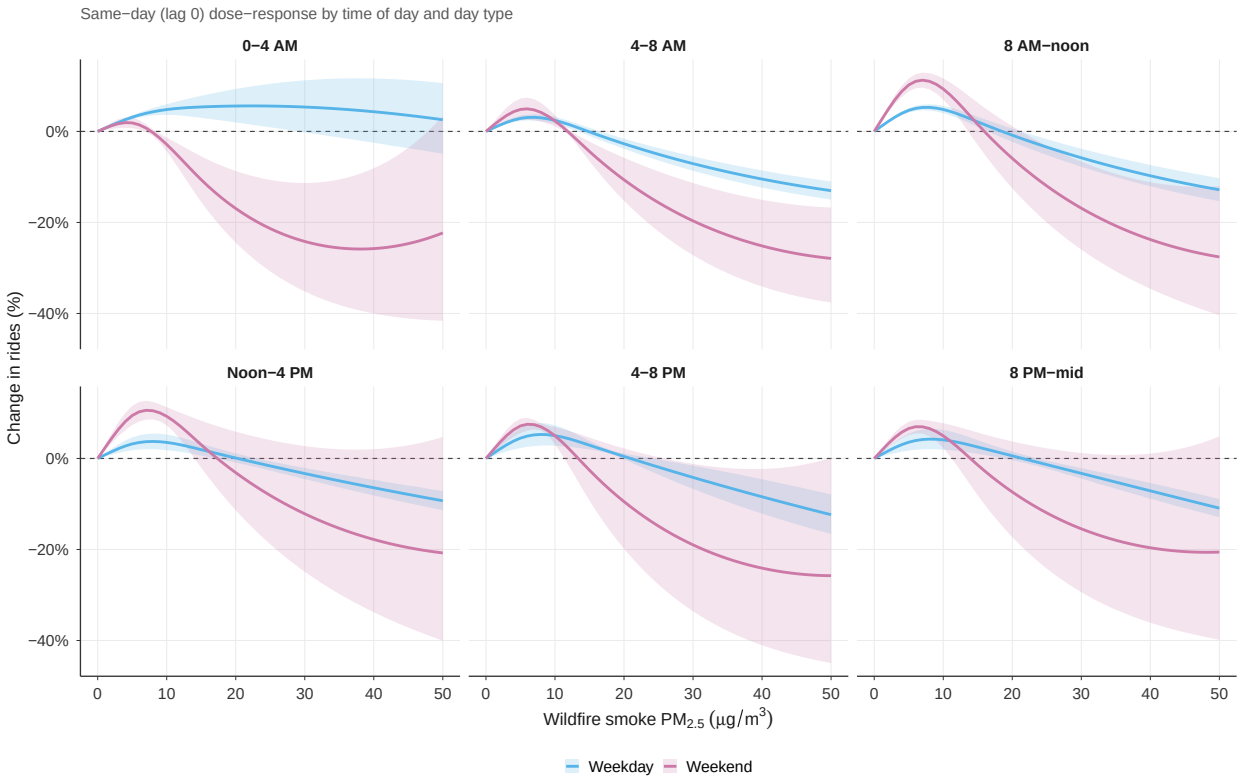

Figure S3: Impacts of wildfire smoke on rides by time of day and weekday or weekend. Exposure-response estimated separately by time-of-day departure window and for weekdays versus weekends. Wildfire smoke reduces ridership across all times of day and both day types, with the largest declines among weekend trips, consistent with recreational travel being more readily deferred than commuting.

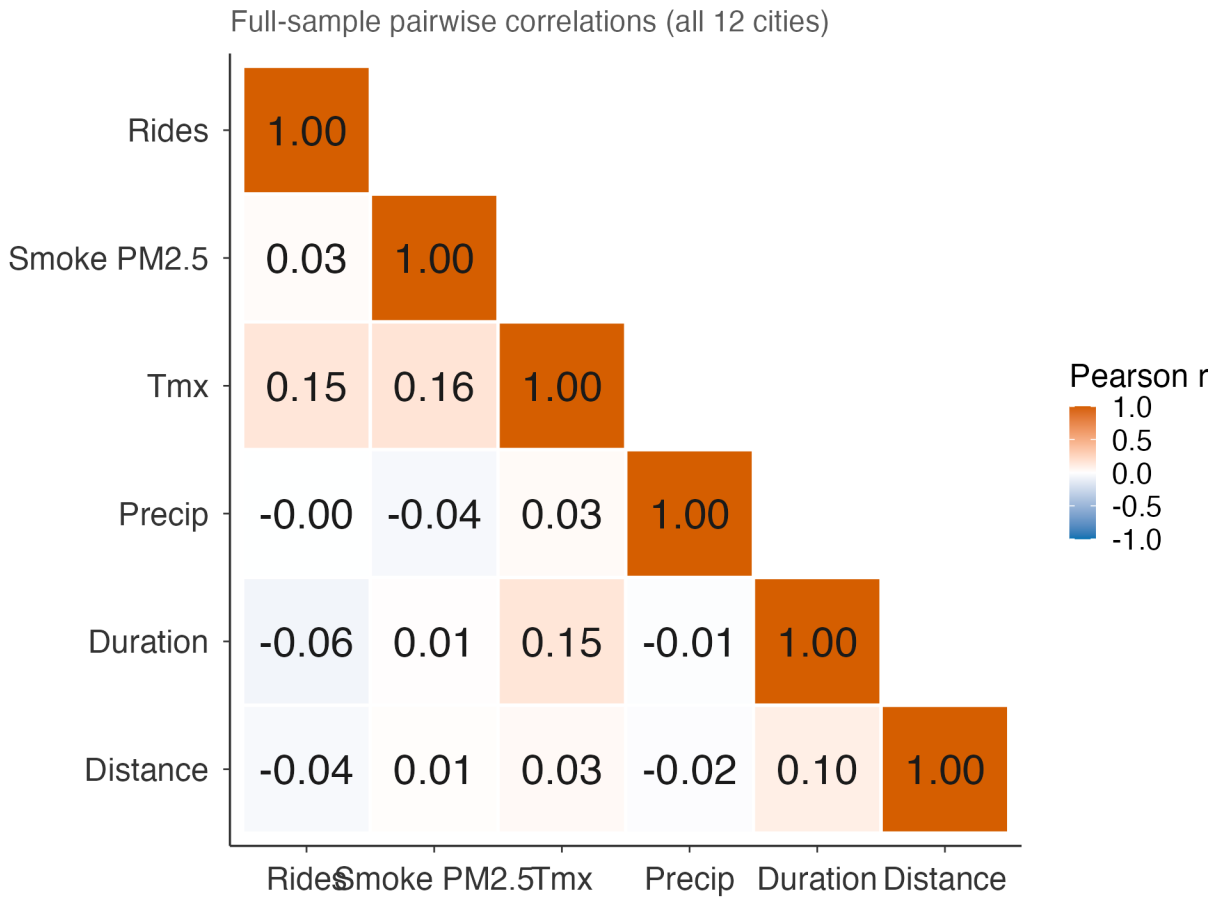

Figure S4: Daily correlations between study variables. Pairwise correlations among daily variables across the estimation sample. Wildfire smoke is positively correlated with temperature and negatively with precipitation; this confounding structure is what our weather controls absorb and what produces the apparent positive association between low smoke and ridership.

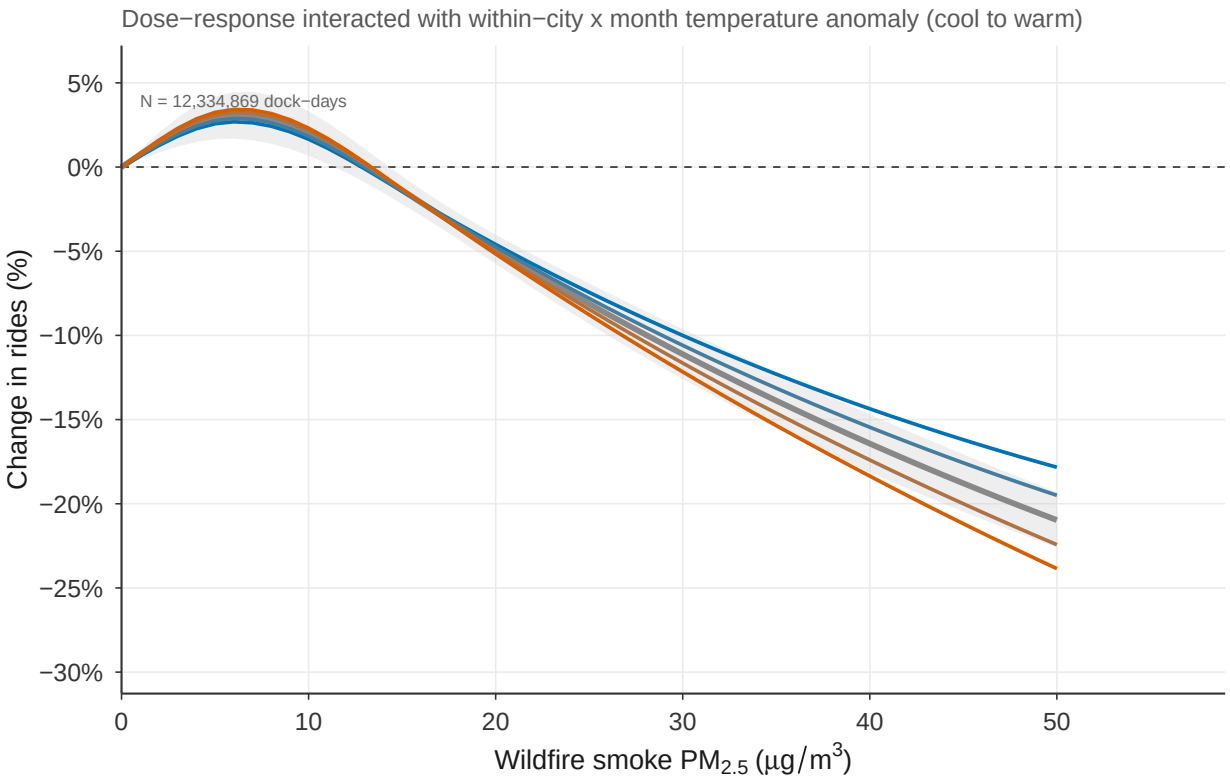

Figure S5: Temperature–smoke interaction. Exposure-response evaluated at temperature quantiles (cool, moderate, warm days). The response is broadly similar across the three, indicating that the smoke effect is distinct from temperature rather than an artifact of hot and smoky days coinciding.

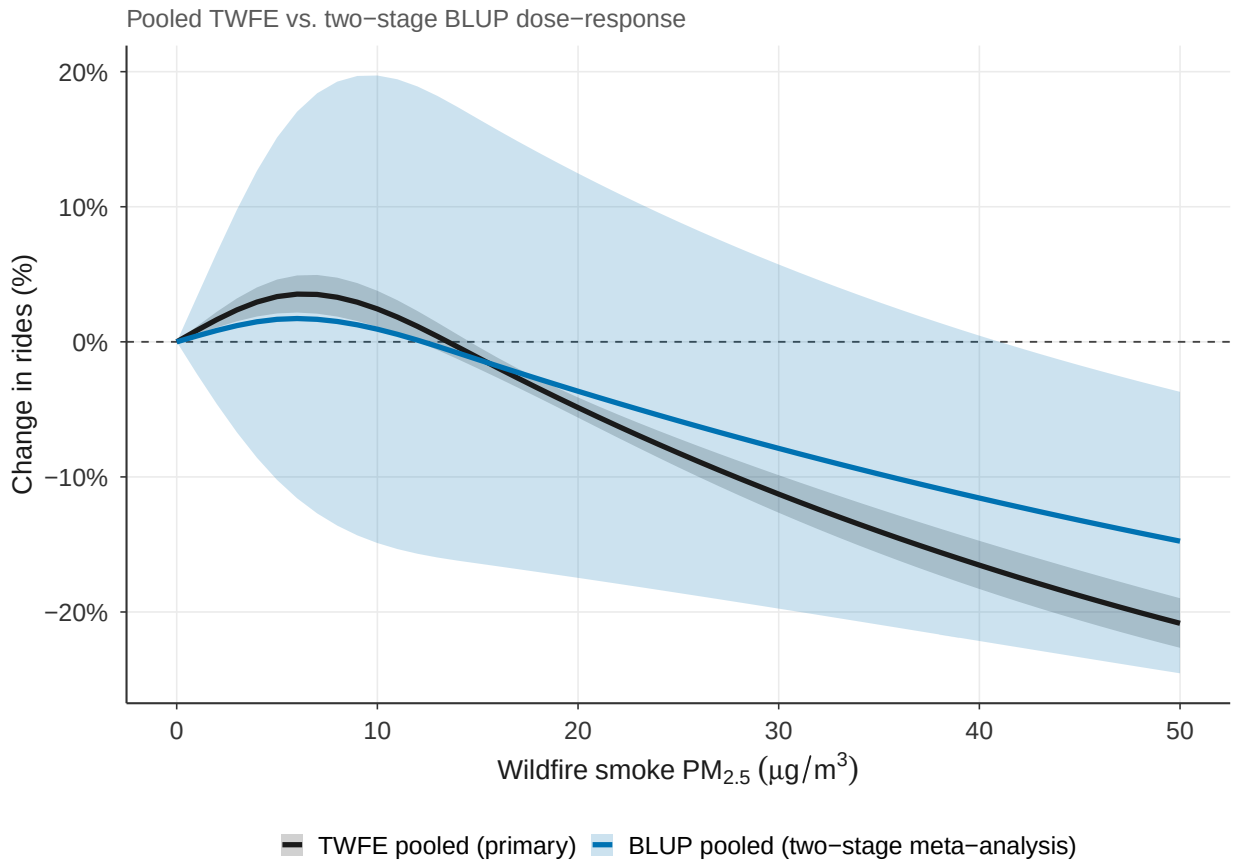

Figure S6: Pooled TWFE vs. two-stage BLUP exposure-response. The BLUP pooled estimate shows wider confidence intervals at low smoke and no positive uptick, reflecting between-city heterogeneity that the single-stage model averages over.

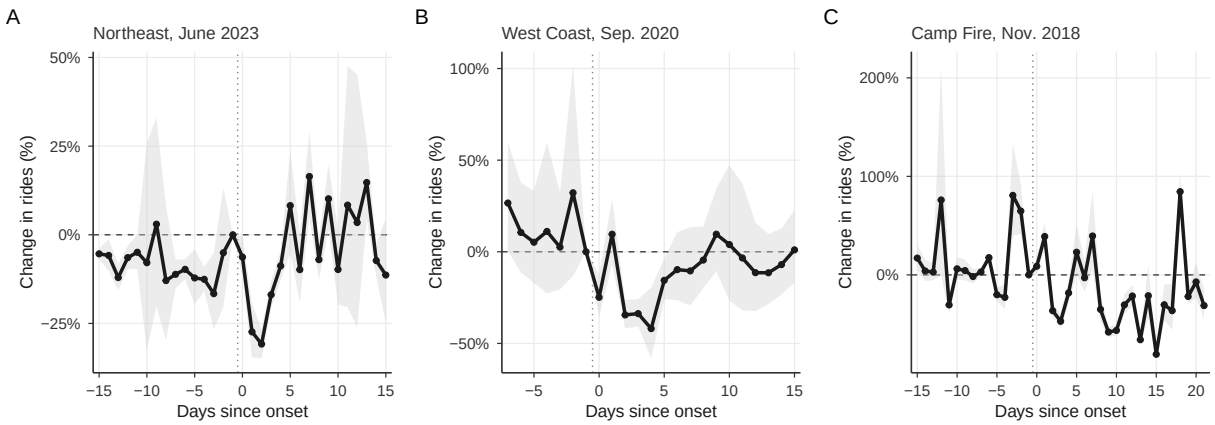

Figure S7: Event studies estimated with two-way fixed effects Poisson DiD (robustness check for main Fig. 4). For each anchor event we estimate $\log \mathbb{E}[n_{idt}] = \sum_{\tau \neq -1} \beta_\tau \cdot \mathbf{1}[t = \tau] \cdot \text{Treated}_i + \gamma X_{dt} + \alpha_i + \delta_t$ at the dock × day level, where dock fixed effects α_i absorb time-invariant station characteristics and date fixed effects δ_t absorb all common shocks within the event window; weather controls X_{dt} match the primary specification, standard errors are clustered by city, and the reference day is $\tau = -1$. Peak single-day declines are −30.8% (day 2) for Northeast 2023 **(A)**, −41.9% (day 4) for West Coast 2020 **(B)**, and −80.6% (day 15) for Camp Fire 2018 **(C)**. The estimator does not require a clean pre-period for counterfactual construction, so it is robust to the short, partially-smoke-contaminated pre-windows that complicate the interactive fixed-effects fit; the peak declines agree closely with the IFE estimates reported in the main text. Camp Fire confidence intervals are wide because a single city (San Francisco) is treated. Shaded regions: 95% confidence intervals clustered by city.

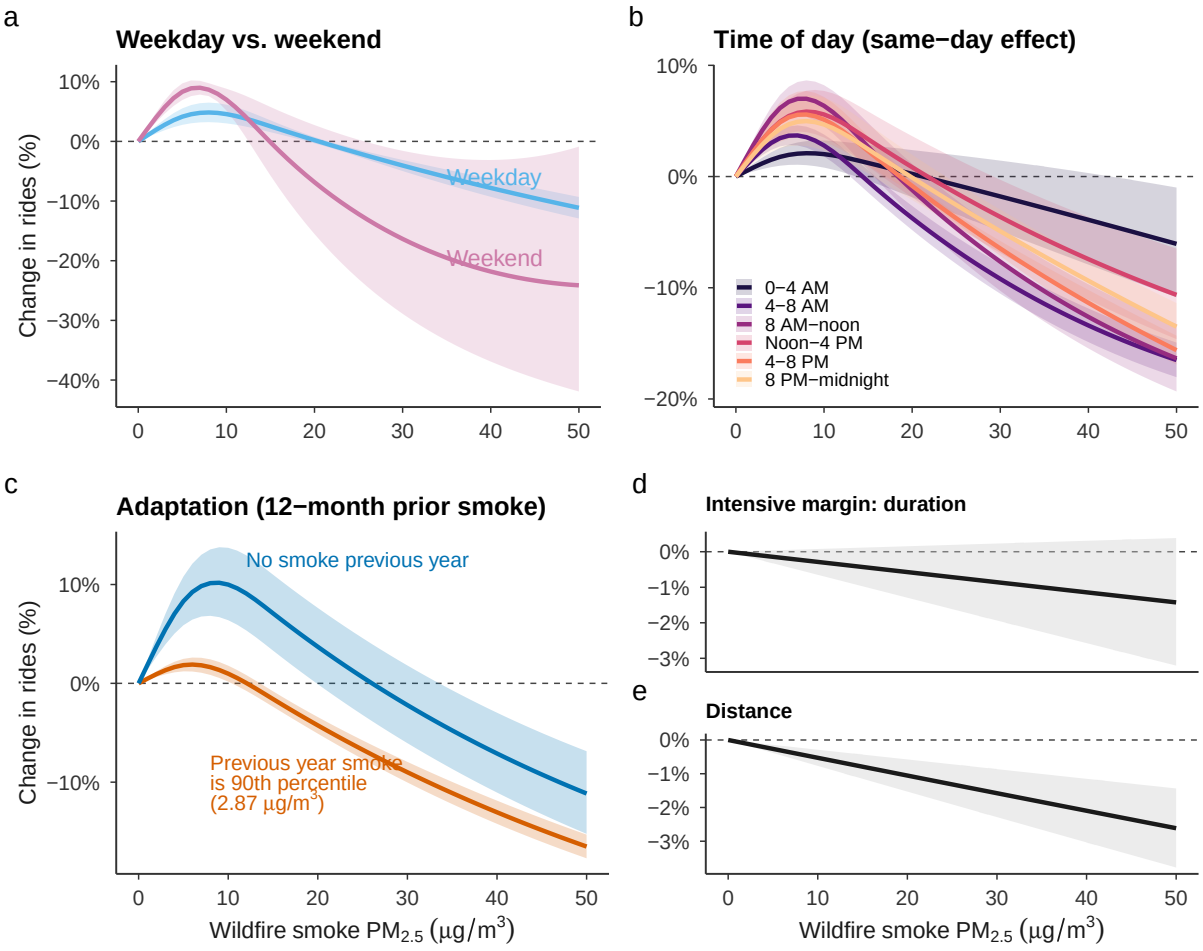

Figure S8: Heterogeneity of bikeshare responses to wildfire smoke on same day ridership. Mirrors main Fig 3 but with the outcome restricted to same-day ridership (lag 0). The same heterogeneity patterns hold, but at smaller magnitudes than the cumulative (lag 0–2) estimates, consistent with most avoidance materializing the day after smoke rather than the same day.

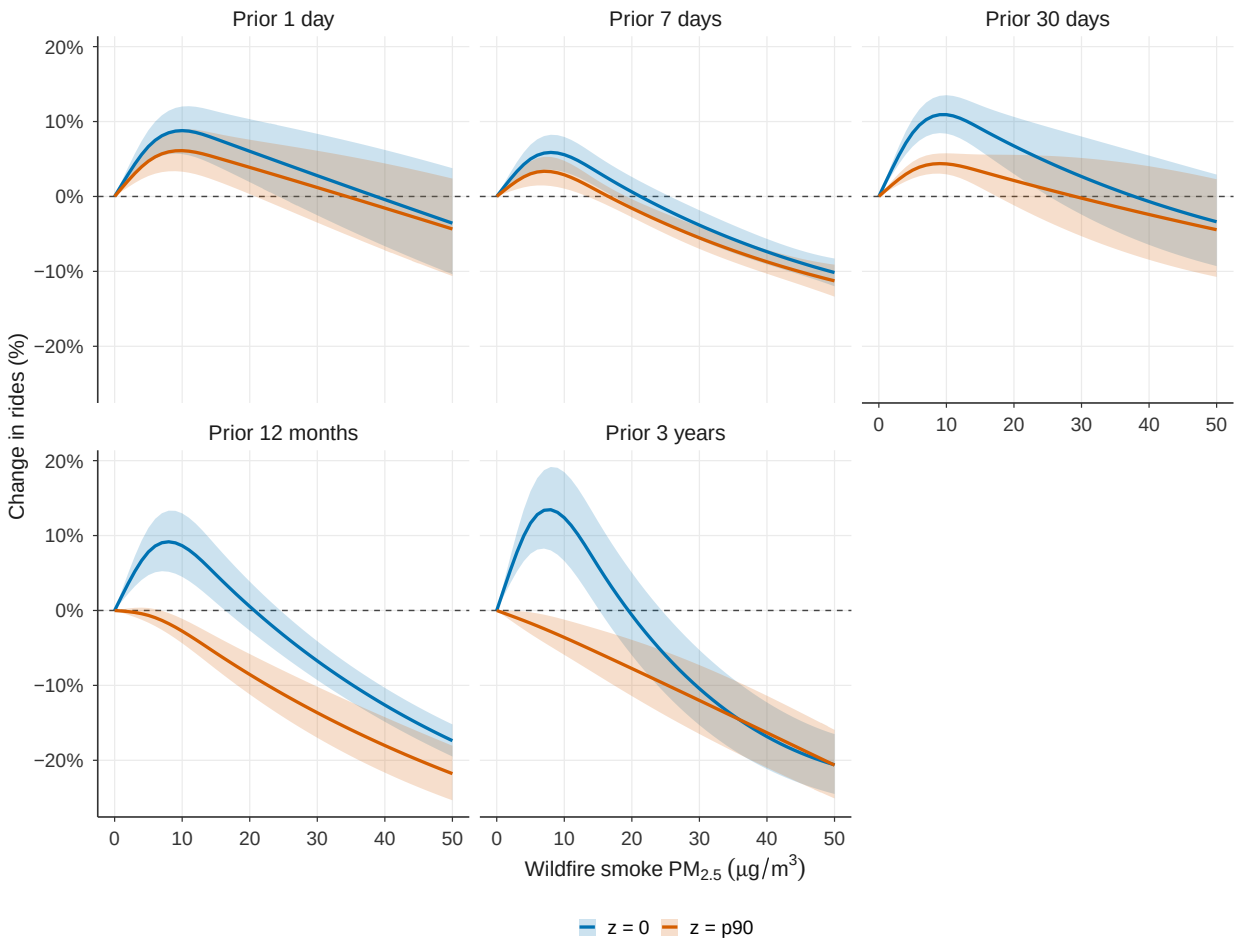

Figure S9: Exposure-response by prior-smoke time horizon. Each panel overlays the estimated exposure-response at zero prior exposure (blue) and the 90th percentile of the modifier (orange). Five time horizons are shown: 1-day, 7-day, 30-day, 12-month, and 3-year rolling averages of prior smoke $PM_{2.5}$. Modification builds over months and peaks at the 12-month horizon (1.9, 1.9, 3.7, 7.9, and 3.9 pp spread at 25 $\mu g/m^3$ for the 1-day, 7-day, 30-day, 12-month, and 3-year modifiers, respectively), consistent with adaptation on a year-over-year timescale. Shaded regions: 95% confidence intervals.

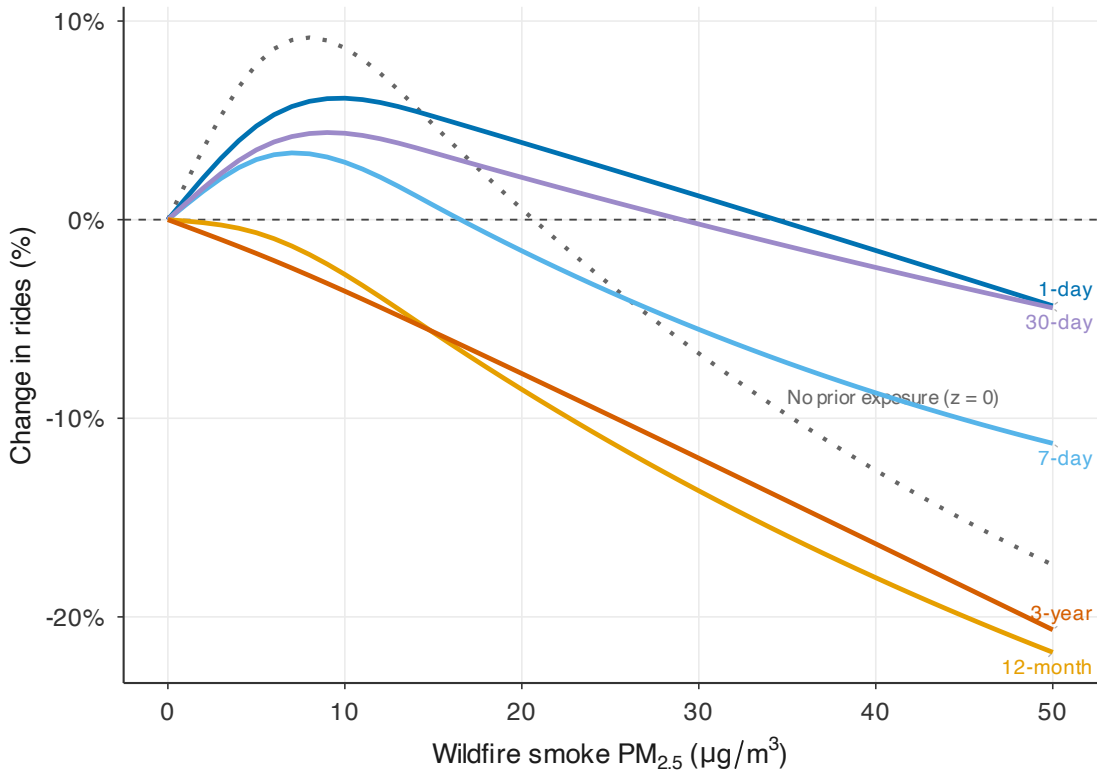

Figure S10: Robustness of the adaptation finding to alternative modifier specifications. Each panel overlays the estimated exposure-response at zero prior exposure (blue) and the 90th percentile of the modifier (orange, with p90 value annotated). Top row: four alternative characterizations of 12-month prior smoke exposure — average concentration (primary specification, 7.9 pp spread at 25 µg/m^3), maximum single-day smoke, total smoke days, and heavy smoke days (>10 µg/m^3). Bottom row: four within-episode tests — yesterday's smoke, consecutive smoke days in the current episode, cumulative smoke over the prior 3 days, and a binary indicator for day 2 or later of an episode. Modification is substantive only for the primary 12-month average concentration. All other specifications produce curves that are nearly indistinguishable. Shaded regions: 95% confidence intervals.

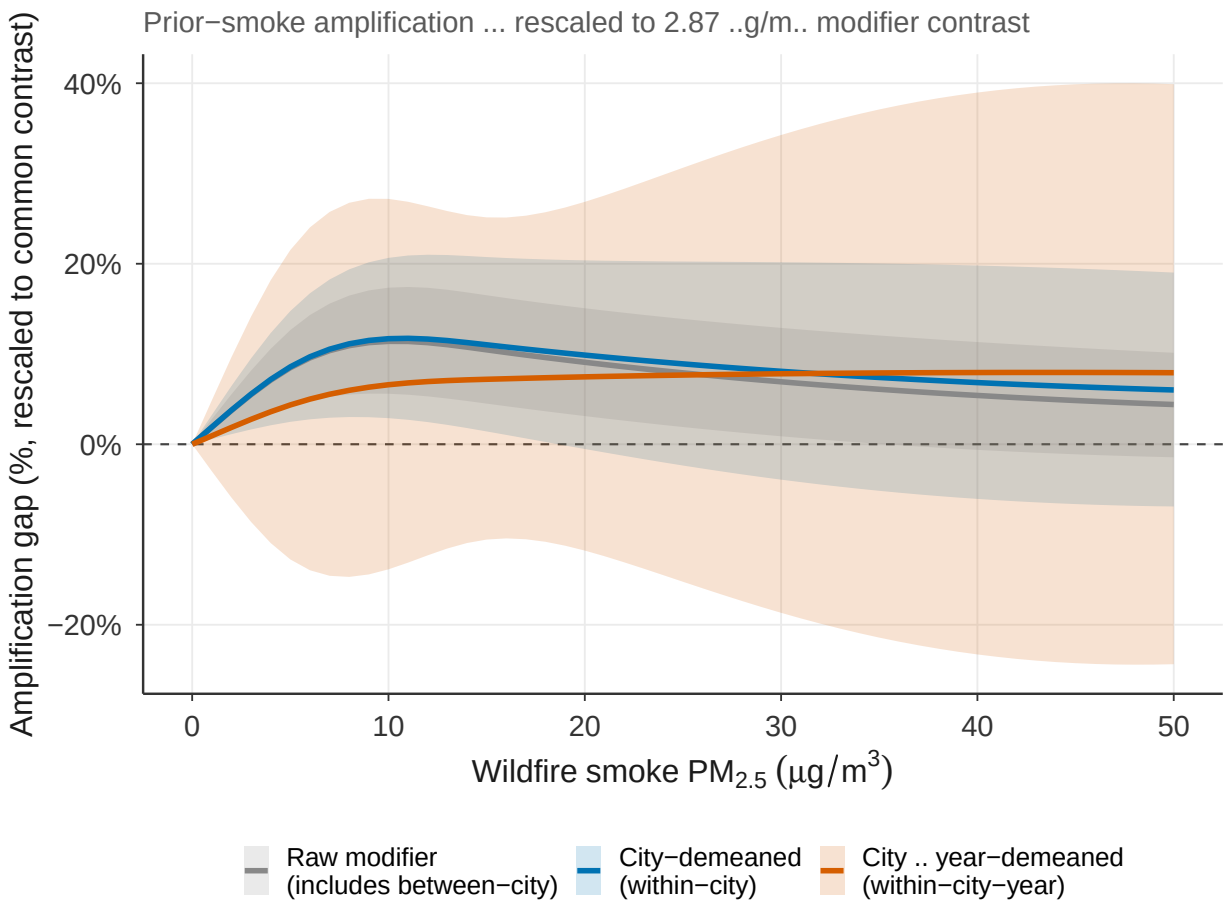

Figure S11: Within-city robustness of the adaptation modifier. Exposure-response at $z = 0$ vs. $z =$ p90 for three modifier versions: original (spread = 7.9 pp at 25 µg/m^3), city-demeaned (5.8 pp), and city×year-demeaned (1.9 pp). The primary signal is between-year within cities.

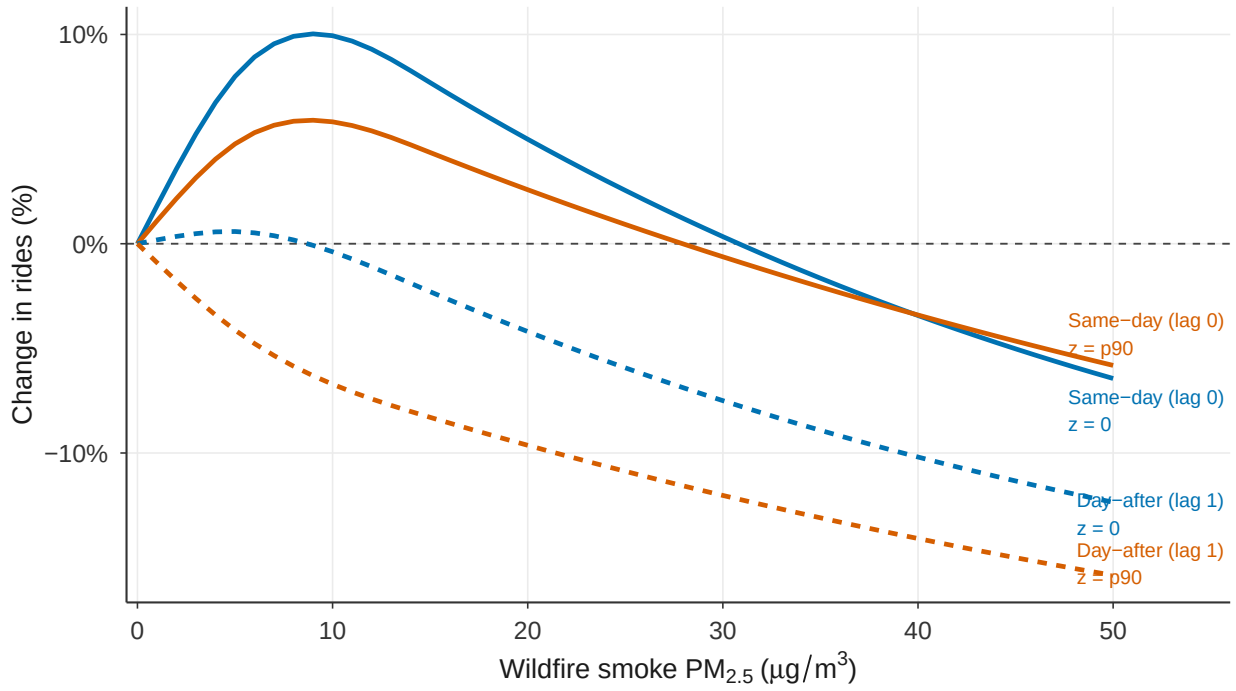

Figure S12: Anticipatory versus reactive avoidance, by prior exposure. Same-day (lag 0, solid) and day-after (lag 1, dashed) components of the smoke exposure-response, each evaluated at zero prior-year exposure (blue) and the 90th percentile of the 12-month modifier (orange). At 25 µg/m^3, the day-after share of the total avoidance response rises from 70% at zero prior exposure to 92% at the 90th percentile: experienced populations shift weight from same-day (reactive) toward day-after (anticipatory) avoidance, consistent with learning to act on air-quality forecasts. Shaded regions: 95% confidence intervals.

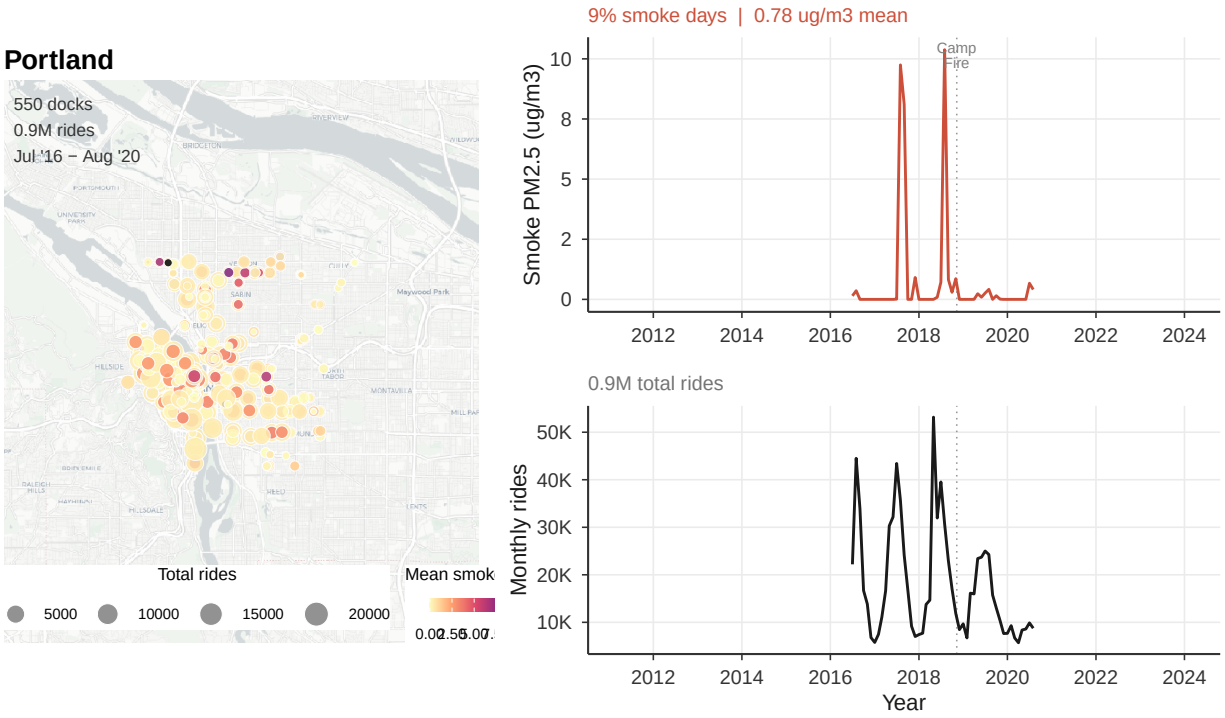

Figure S13: Portland city profile. Left: dock locations sized by total rides and colored by mean wildfire smoke exposure. Right: monthly time series of wildfire smoke $PM_{2.5}$ (top) and total bike-share rides (bottom). Dotted vertical lines mark the Camp Fire (November 2018), Western wildfires (September 2020), and Northeast smoke event (June 2023).

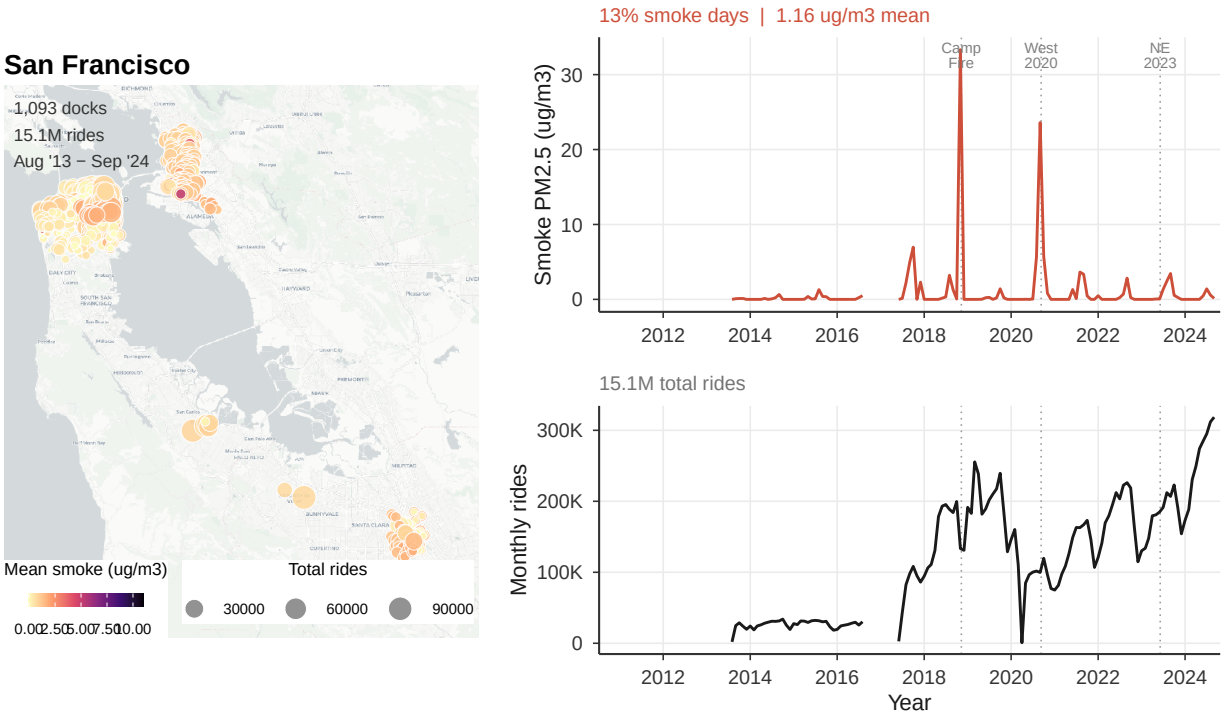

Figure S14: San Francisco Bay Area city profile. The San Francisco system covers the broader Bay Area fleet, with stations in San Francisco, Oakland, and San Jose. Left: dock locations sized by total rides and colored by mean wildfire smoke exposure. Right: monthly time series of wildfire smoke $PM_{2.5}$ (top) and total bikeshare rides (bottom). Dotted vertical lines mark the Camp Fire (November 2018), Western wildfires (September 2020), and Northeast smoke event (June 2023).

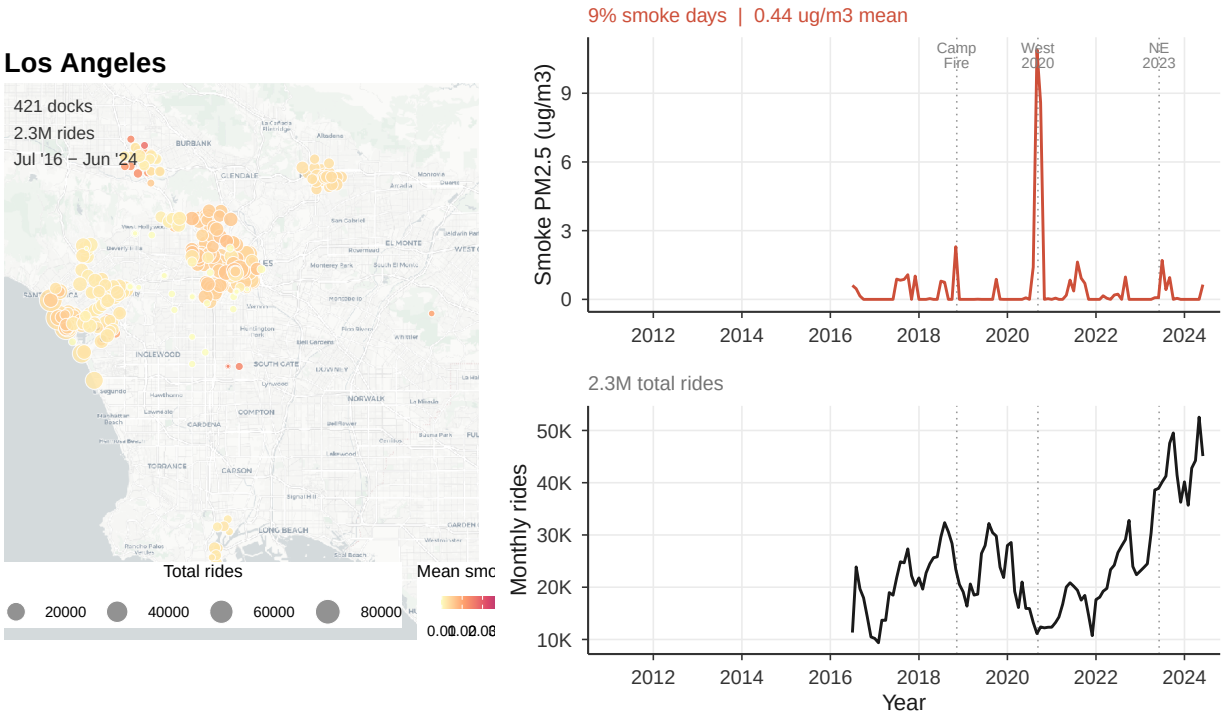

Figure S15: Los Angeles city profile. Left: dock locations sized by total rides and colored by mean wildfire smoke exposure. Right: monthly time series of wildfire smoke $PM_{2.5}$ (top) and total bikeshare rides (bottom). Dotted vertical lines mark the Camp Fire (November 2018), Western wildfires (September 2020), and Northeast smoke event (June 2023).

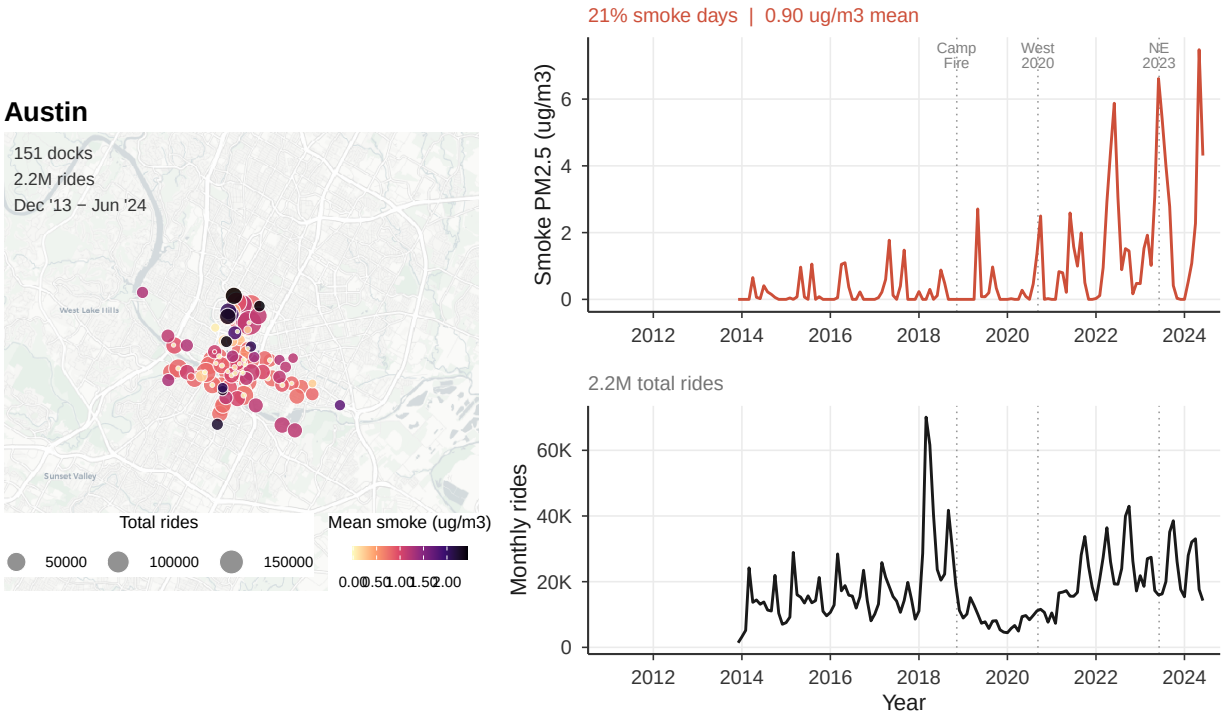

Figure S16: Austin city profile. Left: dock locations sized by total rides and colored by mean wildfire smoke exposure. Right: monthly time series of wildfire smoke $PM_{2.5}$ (top) and total bikeshare rides (bottom). Dotted vertical lines mark the Camp Fire (November 2018), Western wildfires (September 2020), and Northeast smoke event (June 2023).

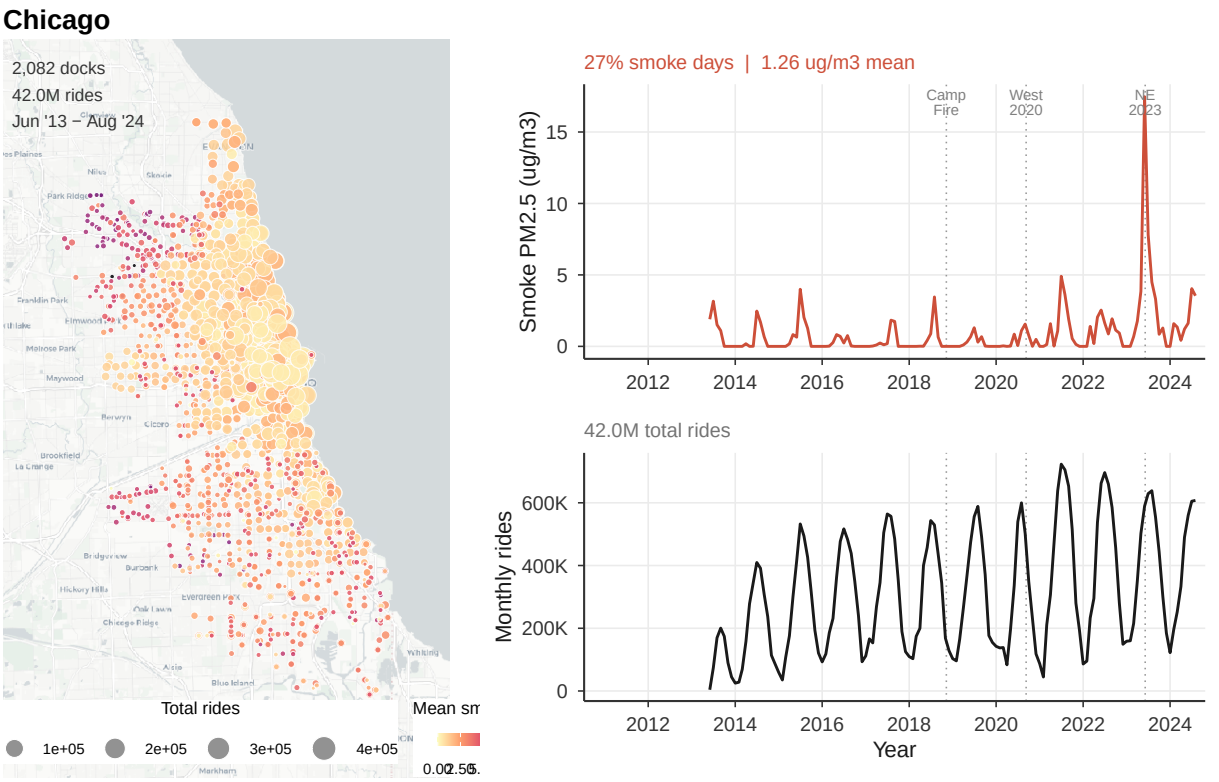

Figure S17: Chicago city profile. Left: dock locations sized by total rides and colored by mean wildfire smoke exposure. Right: monthly time series of wildfire smoke $PM_{2.5}$ (top) and total bike-share rides (bottom). Dotted vertical lines mark the Camp Fire (November 2018), Western wildfires (September 2020), and Northeast smoke event (June 2023).

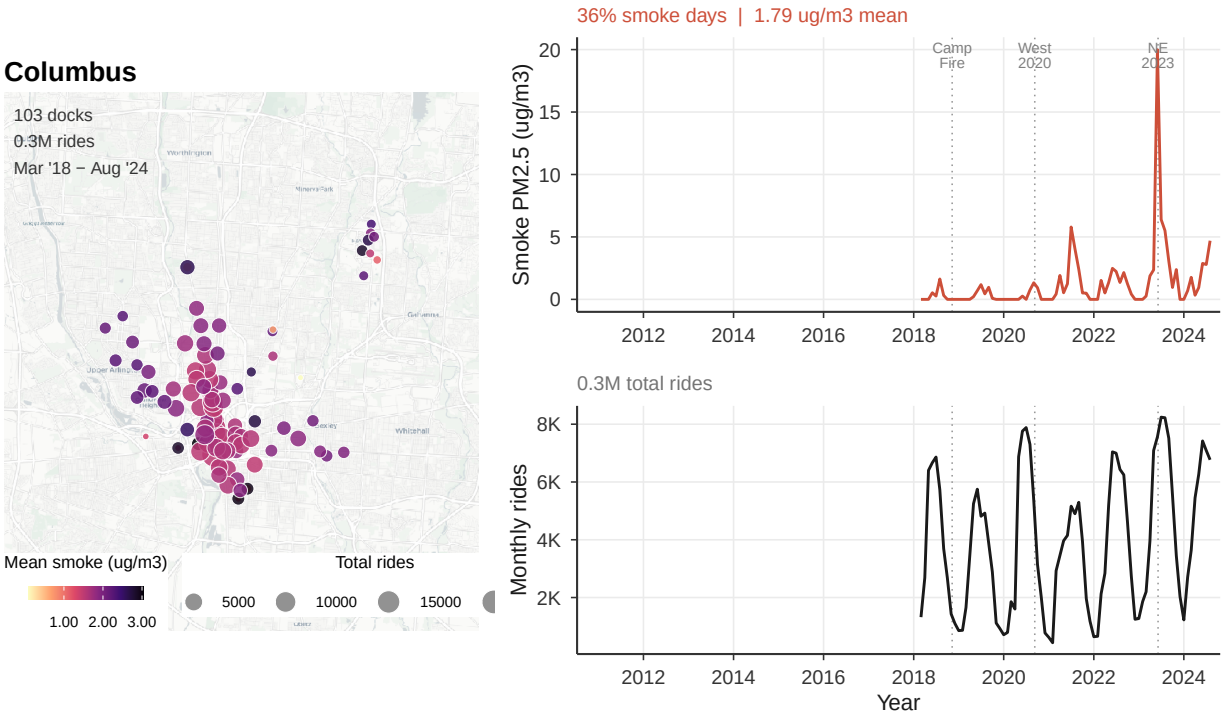

Figure S18: Columbus city profile. Left: dock locations sized by total rides and colored by mean wildfire smoke exposure. Right: monthly time series of wildfire smoke $PM_{2.5}$ (top) and total bike-share rides (bottom). Dotted vertical lines mark the Camp Fire (November 2018), Western wildfires (September 2020), and Northeast smoke event (June 2023).

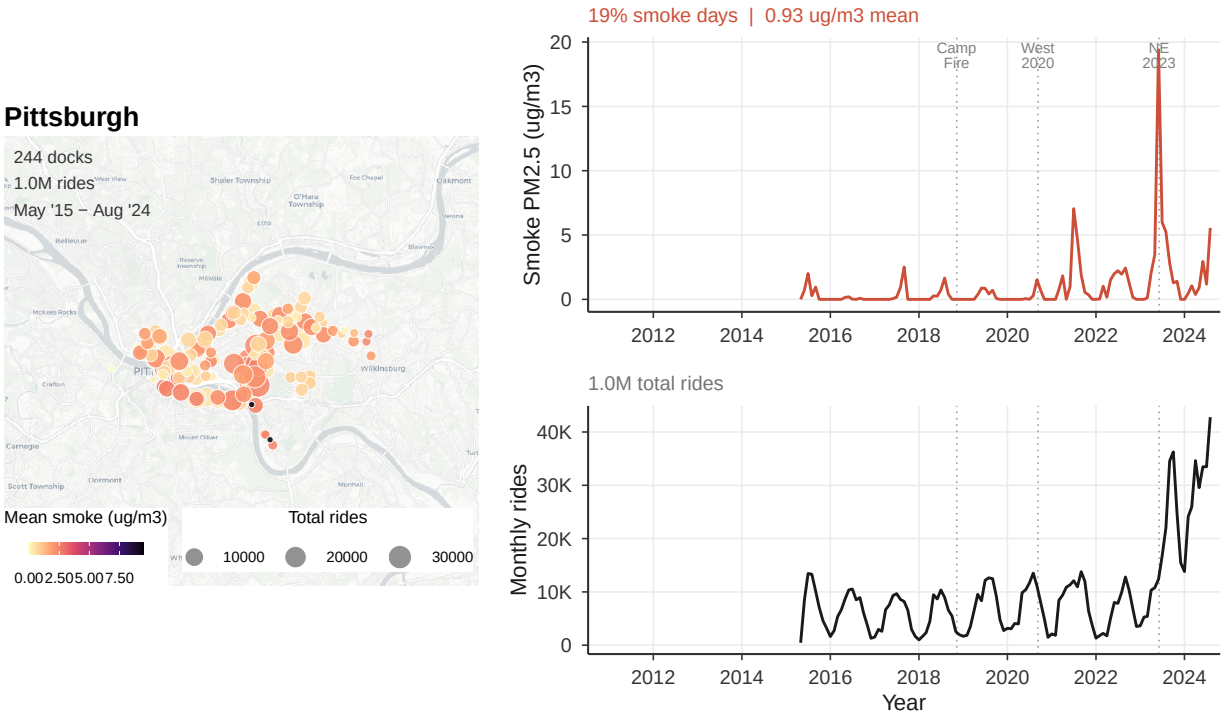

Figure S19: Pittsburgh city profile. Left: dock locations sized by total rides and colored by mean wildfire smoke exposure. Right: monthly time series of wildfire smoke $PM_{2.5}$ (top) and total bike-share rides (bottom). Dotted vertical lines mark the Camp Fire (November 2018), Western wildfires (September 2020), and Northeast smoke event (June 2023).

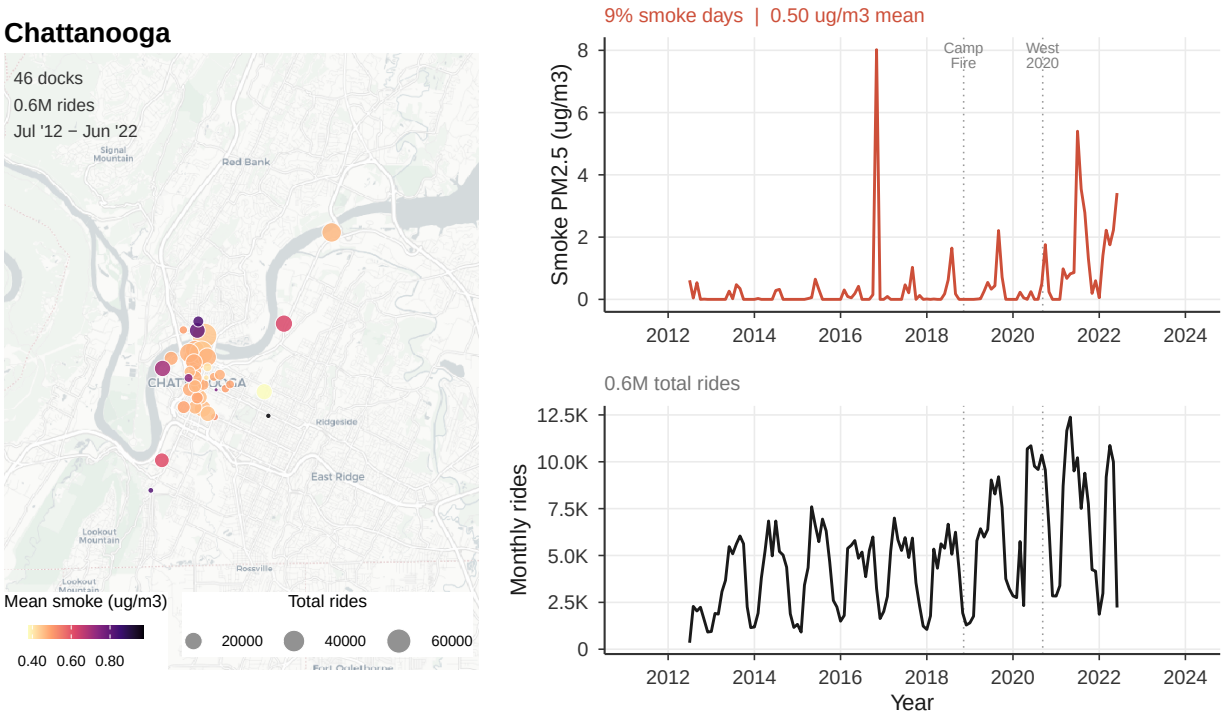

Figure S20: Chattanooga city profile. Left: dock locations sized by total rides and colored by mean wildfire smoke exposure. Right: monthly time series of wildfire smoke $PM_{2.5}$ (top) and total bikeshare rides (bottom). Dotted vertical lines mark the Camp Fire (November 2018) and Western wildfires (September 2020) as reference dates.

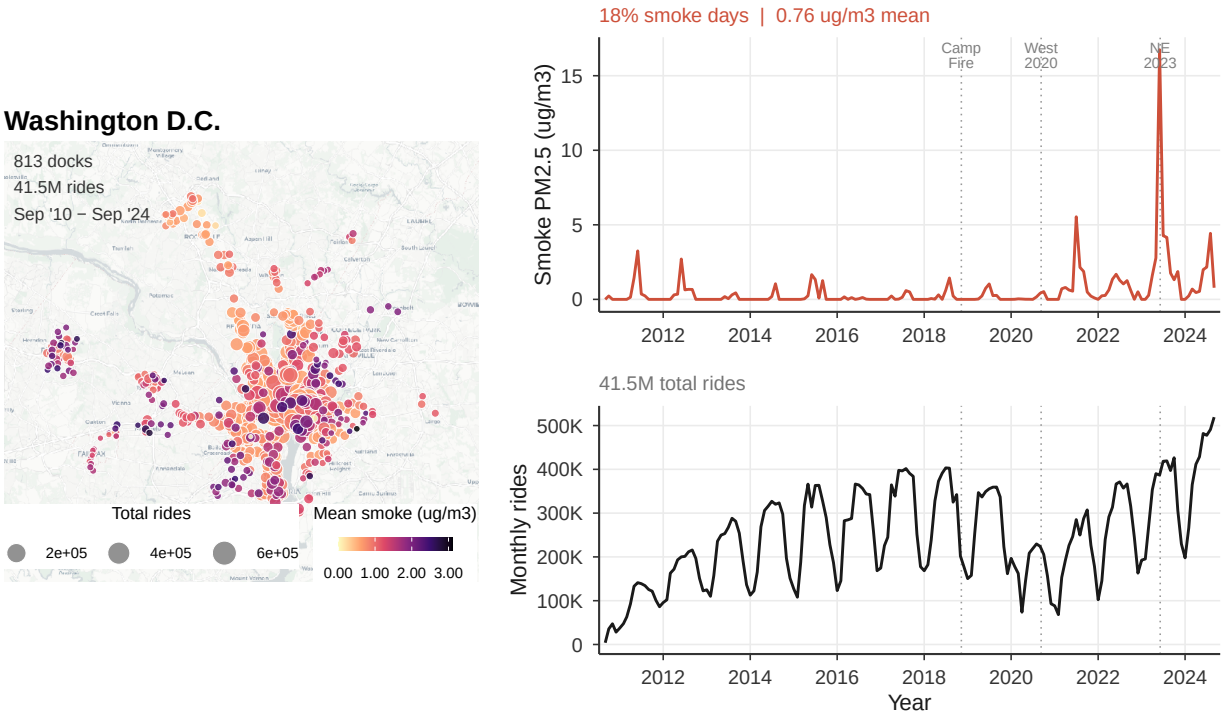

Figure S21: Washington D.C. city profile. Left: dock locations sized by total rides and colored by mean wildfire smoke exposure. Right: monthly time series of wildfire smoke $PM_{2.5}$ (top) and total bikeshare rides (bottom). Dotted vertical lines mark the Camp Fire (November 2018), Western wildfires (September 2020), and Northeast smoke event (June 2023).

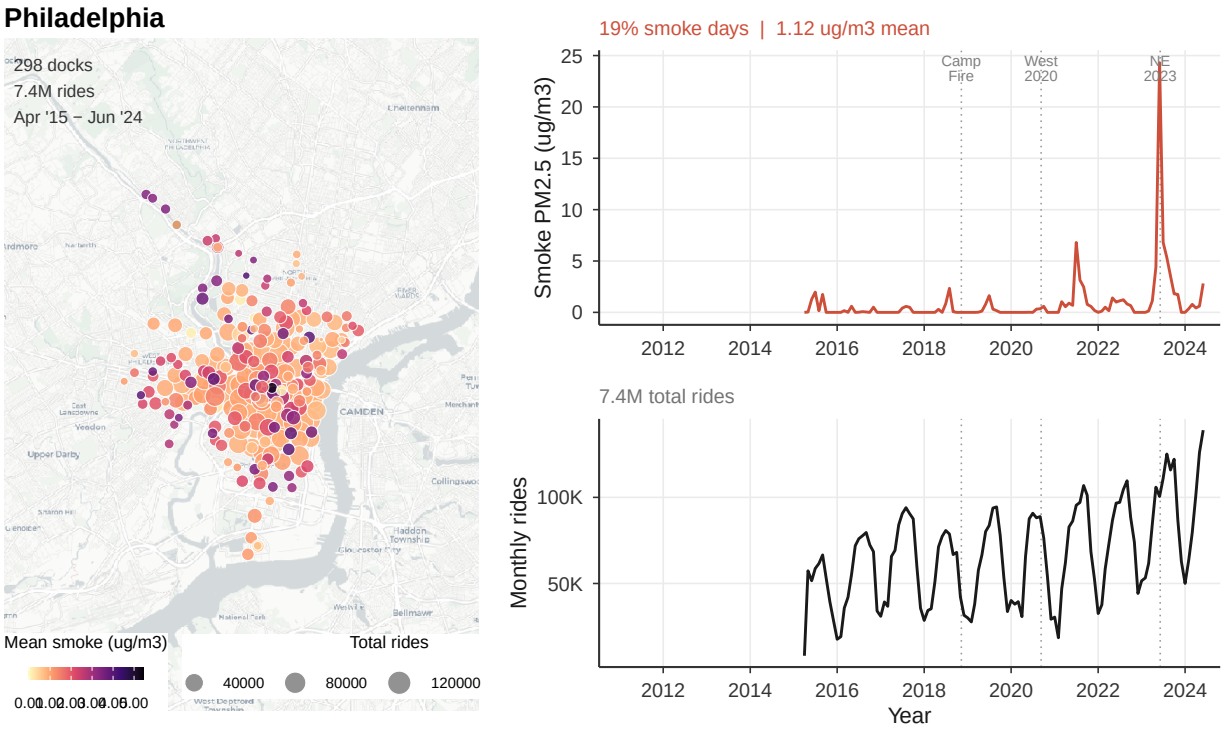

Figure S22: Philadelphia city profile. Left: dock locations sized by total rides and colored by mean wildfire smoke exposure. Right: monthly time series of wildfire smoke $PM_{2.5}$ (top) and total bikeshare rides (bottom). Dotted vertical lines mark the Camp Fire (November 2018), Western wildfires (September 2020), and Northeast smoke event (June 2023).

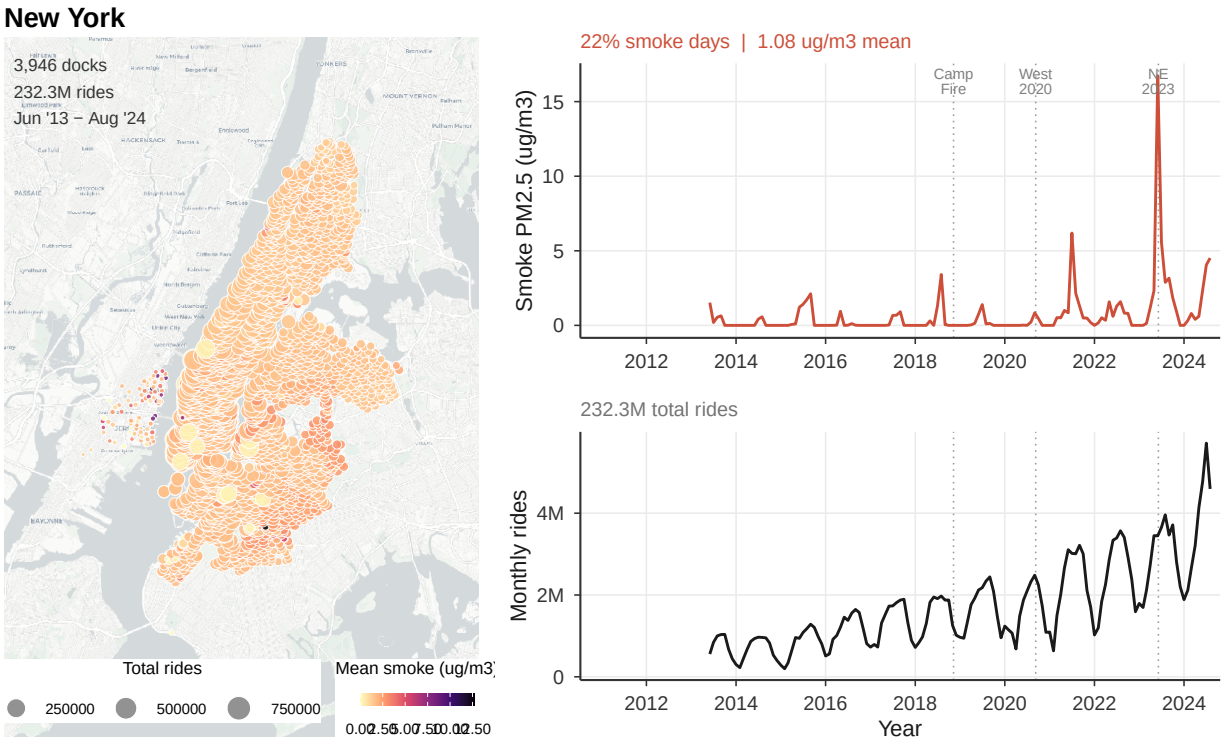

Figure S23: New York city profile. Left: dock locations sized by total rides and colored by mean wildfire smoke exposure. Right: monthly time series of wildfire smoke $PM_{2.5}$ (top) and total bike-share rides (bottom). Dotted vertical lines mark the Camp Fire (November 2018), Western wildfires (September 2020), and Northeast smoke event (June 2023).

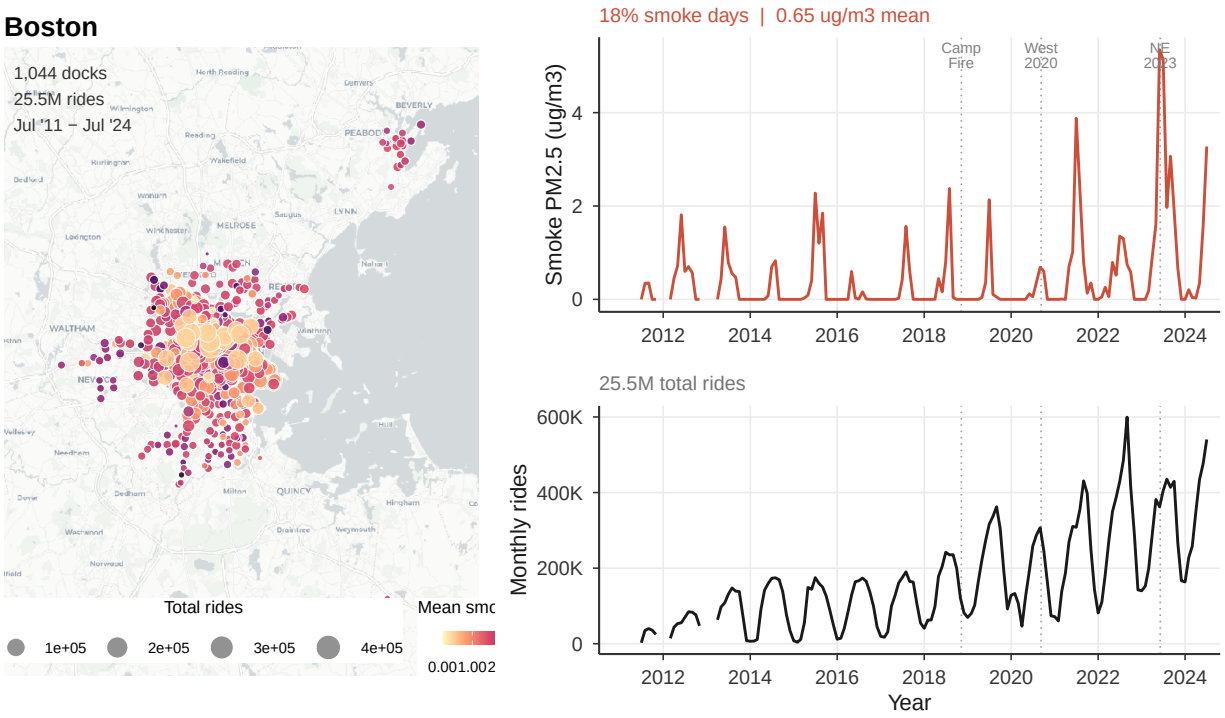

Figure S24: Boston city profile. Left: dock locations sized by total rides and colored by mean wildfire smoke exposure. Right: monthly time series of wildfire smoke $PM_{2.5}$ (top) and total bikeshare rides (bottom). Dotted vertical lines mark the Camp Fire (November 2018), Western wildfires (September 2020), and Northeast smoke event (June 2023).

Table S1: Small-cluster inference: Ibragimov–Müller t-test. For each city, a city-level DLNM (identical specification to the pooled model) is estimated and the cumulative effect at the focal concentration is extracted; a one-sample t_{11} test is then applied to the 12 city-specific estimates, treating each city as one observation. The test is significant at 50 µg/m^3 ($p < 0.001$) but only marginal at 25 µg/m^3 ($p = 0.067$), reflecting the conservatism of inference with just 12 clusters; the primary clustered-SE estimates remain the basis for the headline results.

Concentration	G	Mean effect	SE	t-stat	p-value	95% CI
10 µg/m^3	12	+0.1%	4.1	+0.03	0.98	[−9.0%, +9.2%]
25 µg/m^3	12	−12.0%	5.9	−2.03	0.067	[−25.1%, +1.0%]
50 µg/m^3	12	−26.0%	5.6	−4.63	**<0.001**	[−38.3%, −13.6%]